# NATIONAL ADVISORY COMMITTEE FOR AERONAUTICS

**TECHNICAL NOTE 2767**



## DYNAMICS OF MECHANICAL FEEDBACK-TYPE HYDRAULIC SERVOMOTORS UNDER INERTIA LOAD

By Harold Gold, Edward W. Otto and Victor L. Ransom

Lewis Flight Propulsion Laboratory
Cleveland, Ohio


Washington
August 1952

NATIONAL ADVISORY COMMITTEE FOR AERONAUTICS

TECHNICAL NOTE 2767

# DYNAMICS OF MECHANICAL FEEDBACK-TYPE HYDRAULIC SERVOMOTORS UNDER INERTIA LOADS

By Harold Gold, Edward W. Otto, and Victor L. Ransom

## SUMMARY

An analysis of the dynamics of mechanical feedback-type hydraulic servomotors under inertia loads is developed and experimental verification is presented. This analysis, which is developed in terms of two physical parameters, yields direct expressions for the following dynamic responses: (1) the transient response to a step input and the maximum cylinder pressure during the transient and (2) the variation of amplitude attenuation and phase shift with the frequency of a sinusoidally varying input. The validity of the analysis is demonstrated by means of recorded transient and frequency responses obtained on two servomotors. These data, which were obtained over a wide range of inertia loads, input magnitude, and pressure differential, are presented along with the analytically determined responses. In all cases the calculated responses are in close agreement with the measured responses. The relations presented are readily applicable to the design as well as to the analysis of hydraulic servomotors.

## INTRODUCTION

The servomotor dealt with in this paper is a power amplifying, positioning device of the type used in such applications as control-valve positioners, gun-turret positioners, flight controls, and power-steering devices. The hydraulic servomotor as a device has been known for approximately 100 years. Its application to high-speed machinery, however, appears to be relatively recent. There is, consequently, very little published literature on the dynamics of this servomotor in spite of its long history. Nevertheless, when properly designed, the hydraulic servomotor is particularly suited for high-speed service because of the extremely high force-mass ratios that can be obtained and because the device inherently is heavily damped.

A differential equation for the response to a step input of the hydraulic servomotor with mechanical feedback under an inertia load is

available in the literature (reference 1). This equation (a form of which is derived in the present paper) can be considered to be exact over a fairly representative portion of the response but is not valid in the early part of the transient. Furthermore, under a heavy inertia load the fluid on the driving side of the piston may cavitate, in which case the response cannot be described by a single equation. It is therefore necessary to treat the response of the servomotor in distinct phases.

The basic technique employed in this paper in the analysis of the servomotor is the approximation by one or more linear systems whose individual responses match the behavior of the actual system in definable phases of the response. The several linear systems are then correlated by relating each to the same physical parameters of the system. In this instance, two parameters are all that are required for the correlations. One of these parameters is a direct function of the dimensions of the servomotor and the hydraulic pressure drop across the motor. The second parameter is a function of the magnitude of the disturbance and the mass of the load. By means of this method, analytical expressions are obtained for the following dynamic responses of the servomotor: (1) the transient response to a step input and the maximum cylinder pressure during the transient and (2) the variation of amplitude attenuation and phase shift with the frequency of a sinusoidally varying input.

The validity of the analysis is demonstrated by means of recorded transient and frequency responses that were obtained on both a straight-line and a rotary type of servomotor. These data, which were obtained over a wide range of inertia loads, input magnitude, and pressure differential, are presented along with the analytically determined responses. The investigation was conducted at the NACA Lewis laboratory.

## SYMBOLS

The following symbols are used in this analysis:

| | |
|---|---|
| $A$ | ratio of output amplitude at a given frequency to output amplitude at zero frequency |
| $A_p$ | piston area, sq in. |
| $A_v$ | open area of pilot valve (inlet or discharge side), sq in. |
| $a$ | constant |
| $b$ | constant |

| | |
|---|---|
| C | dimensional constant in fluid-flow equation (95.1 $\frac{\text{sq in.}}{\text{sec}\sqrt{\text{lb}}}$ based on specific gravity of 0.851 and flow coefficient of 0.59) |
| c | constant |
| D | constant |
| E | inertia index (transient response) |
| E' | inertia index (frequency response) |
| $F, F_1, F_2$ | functions |
| $f_1$ | low-frequency band-break frequency, cps |
| $f_2$ | high-frequency band-break frequency, cps |
| $f_3$ | cross-over frequency, cps |
| H | constant |
| h | width of vane, in. |
| i | $\sqrt{-1}$ |
| J | polar moment of inertia, (lb-in.)$(\text{sec}^2)$/radians |
| $L_1$ | inner vane radius of rotary servomotor, in. |
| $L_2$ | outer vane radius of rotary servomotor, in. |
| M | load mass, (lb)$(\text{sec}^2)$/in. |
| $P_1$ | upstream cylinder pressure, lb/sq in. abs |
| $P_2$ | downstream cylinder pressure, lb/sq in. abs |
| $P_d$ | drain pressure, lb/sq in. abs |
| $P_s$ | supply pressure, lb/sq in. abs |
| $\Delta P_p$ | pressure drop across piston, lb/sq in. |
| $\Delta P_v$ | valve pressure drop, lb/sq in. |
| $\Delta P_{v,d}$ | discharge-valve pressure drop, lb/sq in. |
| $\Delta P_{v,i}$ | inlet-valve pressure drop, lb/sq in. |

| | |
|---|---|
| $Q$ | shaft torque, lb-in. |
| $q$ | flow through valve, cu in./sec |
| $R$ | ratio of valve travel to piston travel at fixed input, in./in. |
| $r$ | ratio of valve travel to vane shaft rotation at fixed input, in./radians |
| $S$ | magnitude of step (measured at output), in. |
| $S'$ | amplitude of output sine wave at zero frequency, in. |
| $T$ | no-load time constant, sec |
| $t$ | time from start of transient, sec |
| $t_1$ | value of $t$ at inflection point of transient, sec |
| $t_2, t_3$ | value of $t$ at phase limits in transient, sec |
| $W$ | width of valve port (measured perpendicular to line of valve travel), in. |
| $x$ | instantaneous position of output measured from position at $t = 0$, in. |
| $x_1$ | value of $x$ at inflection point of transient response, in. |
| $x_2, x_3$ | value of $x$ at phase limits in transient, in. |
| $x_m$ | value of $x$ at point of maximum deceleration in transient response, in. |
| $\alpha$ | instantaneous position of output measured from position at $t = 0$, radians |
| $\theta$ | magnitude of step (measured at output), radians |
| $\theta'$ | amplitude of output sine wave at zero frequency, radians |
| $\Phi$ | phase shift, radians |
| $\omega$ | angular frequency, radians/sec |
| $\omega_1$ | low-frequency band-break frequency, radians/sec |

$\omega_2$ high-frequency band-break frequency, radians/sec

$\omega_3$ cross-over frequency, radians/sec

## DEFINITIONS AND INITIAL ASSUMPTIONS

Straight-line servomotor. - The elements of the straight-line hydraulic servomotor are shown schematically in figure 1(a). In the neutral position, the spool member of the pilot valve closes the passages to the piston. When the spool member is displaced from the neutral position by movement of the input lever at point A, the flow of fluid through the pilot valve causes the piston to move in the direction which returns the spool to the neutral position. It follows from the geometry of the linkage that for every position of the linkage point A there is a corresponding equilibrium position of the piston. The description of several other forms of pilot valving and feedback linkage is available in the literature.

Rotary servomotor. - The rotary servomotor is shown schematically in figure 1(b). Rotation of the pilot valve with respect to the output shaft opens a pressure passage to one side of the vane and a drain passage to the opposite side of the vane. The vane is thereby caused to rotate in the same direction as the pilot valve. In the neutral position of the valve the passages to either side of the vane are closed.

Initial assumptions. - The analysis which follows is developed with the following initial assumptions:

(1) The area of opening of the pilot valve varies linearly with the motion of the load.

(2) At all positions of the pilot valve the inlet and discharge openings are equal.

(3) At fixed input, the ratio of pilot-valve travel to piston travel is constant.

(4) The supply and drain pressures are constant.

(5) Structure and linkage are rigid.

(6) The compressibility and mass of the hydraulic fluid are negligible.

(7) Mechanical friction forces are negligible.

(8) Leakage is negligible.

(9) Fluid friction losses in the motor passages are negligible.

## TRANSIENT RESPONSE TO A STEP INPUT

The transient response is analyzed for the no-load case as well as for the inertia-load case. The analysis of the response at no load yields an important parameter used in the analysis of the response under an inertia load.

### No-Load Response

Basic character of response. - Under the conditions of zero load on the output shaft and negligible piston and shaft mass, the pressure drop across the piston will be zero during the transient as well as in steady state. In the transient state, therefore, the fluid flow through the cylinder is essentially unobstructed. On the basis of the initial assumptions and on the further assumption of constant flow coefficient of the pilot valve, the flow of fluid is then proportional to the valve opening and hence proportional to the position error of the piston. The velocity of the piston is therefore proportional to the error. This relation between the piston velocity and the error may be expressed by the following equation:

$$T\dot{x} = (S - x) \tag{1}$$

The solution of equation (1) is:

$$x = S\left(1 - e^{-\frac{t}{T}}\right) \tag{2}$$

In the no-load case the transient response is therefore defined by the time constant T.

Determination of time constant from servomotor dimensions (straight-line servomotor). - In the no-load case the sum of the pressure drops across the inlet and discharge ports is equal to the pressure difference across the servomotor. From the initial assumptions it therefore follows that the pressure drops across the two valves are the same and hence equal to half the pressure difference across the servomotor

$$\Delta P_v = \frac{P_s - P_d}{2} \tag{3}$$

If the flow coefficient of the pilot valve is considered constant, the rate of fluid flow into the cylinder is given by the relation

$$q = CA_v\sqrt{\frac{P_s - P_d}{2}} \tag{4}$$

The area of opening of the valves is proportional to the error and may be written

$$A_v = (S - x)RW \tag{5}$$

The velocity of the piston is determined by the flow rate through the valves and is related by the following expression:

$$A_p\dot{x} = q \tag{6}$$

Equations (4), (5), and (6) may be combined to form the differential equation of the response

$$A_p\dot{x} = \left(CRW\sqrt{\frac{P_s - P_d}{2}}\right)(S - x) \tag{7}$$

Equation (7) is of the same form as equation (1), from which it follows that

$$T = \frac{\sqrt{2}\,A_p}{CRW\sqrt{P_s - P_d}} \tag{8}$$

Determination of time constant from motor dimensions (rotary servomotor). - The area of opening of the valves as a function of the error may be written

$$A_v = (\theta - \alpha)rW \tag{9}$$

The angular velocity of the output shaft may be related to the flow rate through the valves by the following expression

$$\frac{h}{2}(L_2^2 - L_1^2)\dot{\alpha} = q \tag{10}$$

Equations (4), (9), and (10) may be combined to form the differential equation of the response

$$\frac{h}{2}(L_2^2 - L_1^2)\dot{\alpha} = \left(CrW\sqrt{\frac{P_s - P_d}{2}}\right)(\theta - \alpha) \tag{11}$$

From equation (11) the time constant is

$$T = \frac{h(L_2^2 - L_1^2)}{\sqrt{2}\, CrW\sqrt{P_s - P_d}} \tag{12}$$

Experimental responses. - A typical response of a hydraulic servomotor to a step input at no load is presented in figure 2. The servomotor used in this run is of the rotary type. The data are plotted as the logarithm of the characteristic term $\left(1 - \frac{\alpha}{\theta}\right)^{-1}$ against time. In a response described by equation (2) (rewritten in terms of $\alpha$ and $\theta$), the term $\log \left(1 - \frac{\alpha}{\theta}\right)^{-1}$ varies linearly with time. The data as shown fall essentially along a straight line and are in close agreement with the calculated response based on the calculated time constant. The calculated response is based on the value of time constant computed by means of equation (12). The dimensions of the servomotor necessary for the application of equation (12) are given in appendix A; also described are the experimental methods used to obtain the data.

In figure 2 the deviation of the data points from the theoretical straight line is the greatest in the early part of the transient where the effect of the internal servomotor mass is greatest. The response in the later part of the transient is less affected by the internal mass and is therefore indicative of the theoretical no-load response. The close agreement of the points with the theoretical straight line over the entire transient can be attributed to the relatively small internal mass of this servomotor. The ratio of static torque to the moment of inertia of the motor in this case was 3,500,000 radians per second per second.

## Transient Response Under Inertia Load

General characteristics of response. - Under the condition of an inertia load on the output shaft, the pressure drop across the piston will be proportional to the acceleration of the load. The general nature of the variation of the pressure drop across the piston along with the corresponding output shaft response is shown in figure 3. In the figure the following relations exist among the cylinder pressures $P_1$ and $P_2$ and the pressure drops across the piston $\Delta P_p$, the inlet valve $\Delta P_{v,i}$, and the discharge valve $\Delta P_{v,d}$:

$$\Delta P_p = P_1 - P_2$$

$$\Delta P_{v,i} = P_s - P_1$$

$$\Delta P_{v,d} = P_2 - P_d$$

In the steady state, the pressure drop across the piston is zero. The cylinder pressures are equal and their magnitude is a function of the leakage areas around the valves. If the leakage areas around the valves are equal, the cylinder pressures will be equal to $(P_s - P_d)/2$. This condition is assumed in figure 3.

In response to a step input, $P_1$ immediately rises to the supply pressure $P_s$, and $P_2$ immediately drops to the drain pressure $P_d$. The accelerating pressure differential is then initially $(P_s - P_d)$. As the piston accelerates, the flow of fluid through the valve ports increases and at the same time the valve-port areas decrease. This action causes $P_1$ to decrease and $P_2$ to increase. The two curves $(P_1 = F_1(t)$ and $P_2 = F_2(t))$ are mirror images and therefore intersect at the value of $(P_s - P_d)/2$. At the intersection, the pressure differential across the piston is zero and the transient is therefore at the inflection point. Beyond the point of intersection of the two pressure curves the momentum of the load causes $P_1$ to continue to decrease and $P_2$ to continue to increase, which action results in a decelerating pressure differential across the piston. The deceleration causes a reduction in the rate of fluid flow through the valves and a consequent reduction in the rate of change of $P_1$ and $P_2$. The pressures $P_2$ and $P_1$ therefore pass through maximum and minimum values, respectively. The deceleration continues until the error is reduced to zero. The magnitude of the maximum and minimum values of the cylinder pressures during the deceleration phase is a function of the value of error and of momentum at the inflection point. Based on these factors alone, the value of the maximum and minimum is finite but not limited. The pressure $P_1$, however, is physically limited at absolute zero. The effect of $P_1$ limited at absolute zero is treated in a later section. In the analysis that follows, the minimum value of $P_1$ is not limited.

In the transient response treated in this section, $P_1$ and $P_2$ vary as mirror images throughout the entire transient. In this case

$$\Delta P_{v,i} = \Delta P_{v,d}$$

The sum of the valve pressure drops may be written

$$\Delta P_{v,i} + \Delta P_{v,d} = 2\Delta P_v$$

The pressure drop across the piston may be written

$$\Delta P_p = P_s - P_d - 2\Delta P_v \tag{13}$$

The pressure drop across the piston is related to the acceleration by the following expression

$$\Delta P_p = \frac{M}{A_p} \ddot{x} \tag{14}$$

From equations (13) and (14)

$$\Delta P_v = \frac{1}{2}\left(P_s - P_d - \frac{M}{A_p} \ddot{x}\right) \tag{15}$$

With the flow coefficient of the pilot valve considered constant, the equation of flow through the valve ports is

$$A_p \dot{x} = \left[CRW\sqrt{\frac{1}{2}\left(P_s - P_d - \frac{M}{A_p} \ddot{x}\right)}\right](S - x) \tag{16}$$

Equation (16) cannot be integrated to $x$ except by numerical or graphical methods. Some solutions of equation (16) are given in reference 1.

Under an inertia load the piston is accelerated from zero velocity. There is consequently an initial period in the response during which the flow through the valve ports is laminar. As a result of this, the flow coefficient of the pilot valve is not constant but is subject to wide variation. The net effect of the variation in flow coefficient is that of a marked reduction, which results in slower initial acceleration rate than is indicated by equation (16). This effect is apparent in the comparison between measured responses and responses calculated by a form of equation (16) shown in reference 1.

At the conclusion of the transient the piston velocity again approaches zero, but in this part of the transient the valve areas also approach zero so that high fluid velocity is maintained in the valve ports. The flow coefficient may therefore be considered constant except in the initial acceleration phase. In the no-load case the assumption of constant-flow coefficient is valid because the piston velocity is a maximum at the start of the transient.

In spite of the complex nature of the response there are basically only two phases in the transient: the acceleration phase and the deceleration phase. This conclusion, particularly with reference to a continuous deceleration phase without overshoot or oscillation, is based on the assumption of rigid oil and structure and zero leakage. Figure 4 shows an oscillographic record of the response of a servomotor to a step input under a relatively heavy inertia load. The characteristic acceleration phase and dead-beat deceleration phase are quite clearly demonstrated.

Linear system for approximation of acceleration phase of transient response. - It is indicated by the measured responses of hydraulic servomotors under inertia loads that the acceleration phase may be approximated by a linear second-order system. The general form of a second-order differential equation with constant coefficients may be written

$$a\ddot{x} + b\dot{x} + x = c \tag{17}$$

The constants a, b, and c are now evaluated to match the physical system.

The equilibrium value of x in the physical system has been defined by the symbol S; hence,

$$c = S$$

At no load the servomotor responds as a first-order system. Equation (17) should therefore reduce to equation (1) for the inertialess case. Therefore,

$$b = T$$

The constant a can be determined from the initial conditions.

When

$$t = +0$$

$$x = 0$$

$$\dot{x} = 0$$

$$\ddot{x} = \frac{(P_s - P_d)A_p}{M} \text{ (see fig. 3)}$$

The substitution of these values in equation (17) yields

$$a = \frac{MS}{(P_s - P_d)A_p} \tag{18}$$

The differential equation of the linear system that approximates the acceleration phase is then

$$\frac{MS}{(P_s - P_d)A_p} \ddot{x} + T\dot{x} + x = S \tag{19}$$

Evaluation of coefficients for rotary servomotors. - The stalled torque of the rotary servomotor is given by the following expression:

$$Q = \frac{(P_s - P_d)(L_2^2 - L_1^2)h}{2} \tag{20}$$

Hence, when

$$t = 0$$

$$\ddot{\alpha} = \frac{(P_s - P_d)(L_2^2 - L_1^2)h}{2J}$$

The term $A_p/M$, which occurs in the case of the straight-line servomotor, is replaced in the case of the rotary servomotor by the terms $h(L_2^2 - L_1^2)/2J$. Replacing terms in equation (18) yields

$$a = \frac{2J\theta}{h(L_2^2 - L_1^2)(P_s - P_d)} \tag{21}$$

The differential equation of the linear system that approximates the acceleration phase in the case of the rotary servomotor is

$$\left[\frac{2J\theta}{h(L_2^2 - L_1^2)(P_s - P_d)}\right] \ddot{\alpha} + T\dot{\alpha} + \alpha = \theta \tag{22}$$

Linear system for approximation of deceleration phase of transient response. - In the deceleration phase of the transient the flow through the valve ports is turbulent; consequently the flow coefficient remains constant and equation (16) may be directly applied.

Rearranging terms of equation (16) and dividing both sides by the term $\sqrt{P_s - P_d}$ yields

$$\left(\frac{\sqrt{2}\,A_p}{CRW\sqrt{P_s - P_d}}\right)\frac{\dot{x}}{S - x} = \sqrt{1 - \frac{M\ddot{x}}{A_p(P_s - P_d)}} \tag{23}$$

Substituting equation (8) in equation (23) yields,

$$T\left(\frac{\dot{x}}{S - x}\right) = \sqrt{1 - \frac{M\ddot{x}}{A_p(P_s - P_d)}} \tag{24}$$

At the start of the deceleration phase the value of $\ddot{x}$ is zero and consequently the right-hand side of equation (24) equals unity. As the transient continues, the value of $\ddot{x}$ increases to a maximum value and then returns to zero. For small inertia loads, the peak deceleration pressure difference across the piston will not exceed the value of the term $(P_s - P_d)$ (see fig. 3). In a transient in which the maximum decelerating pressure difference across the piston equals the difference $(P_s - P_d)$, the right-hand side of equation (24) has a maximum value of $\sqrt{2}$. In even extremely severe transients the maximum value of this term will not exceed 2. High values of the maximum deceleration are associated with short durations. The effect of the decelerating pressure differential will therefore have a small effect on the integrated solutions. In treating the deceleration phase of the position response of the servomotor, therefore, the pressure differences across the servomotor may be neglected. Equation (24) may therefore be reduced to

$$T\left(\frac{\dot{x}}{S - x}\right) = 1 \tag{25}$$

Equation (25) is the same as equation (1). In this linearization, therefore, the deceleration phase of the transient is approximated by an exponential decay.

Application of equations. - Equations (19) and (22), which are used in this analysis to approximate the acceleration phase of the transient, are linear second-order differential equations and may be integrated in terms of several parameters. The no-load time constant T will be employed as a parameter in the integrated solution because this quantity is a direct function of the physical dimensions of the servomotor. The second parameter that will be used is the reciprocal of the damping ratio. This quantity is herein designated the inertia index E. The new term is employed in this paper because the quantity is later applied to equations in which the term "damping ratio" would have no meaning.

Equation (19) expressed in terms of the parameters T and E may be written

$$\frac{T^2E^2}{4}\frac{\ddot{x}}{S} + T\frac{\dot{x}}{S} + \frac{x}{S} = 1 \tag{26}$$

The value of E may be obtained directly from the dimensions of the servomotor, the load mass, and the initial error. Equating like coefficients in equations (19) and (26) gives

$$E = \frac{2}{T}\sqrt{\frac{MS}{(P_s - P_d)A_p}} \tag{27}$$

With the substitution of equation (8) in equation (27) the general expression for E is obtained

$$E = \frac{\sqrt{2}\ CRW\sqrt{MS}}{A_p^{3/2}} \tag{28}$$

With the same procedure followed in the case of the rotary servomotor, the inertia index is

$$E = \frac{4CrW\sqrt{\theta J}}{\left[h(L_2^2 - L_1^2)\right]^{3/2}} \tag{29}$$

The integrated forms of equation (26) are as follows:

When E = 1,

$$\frac{x}{S} = 1 - e^{-\left(\frac{2t}{T}\right)}\left[1 + \left(\frac{2}{T}\right)t\right] \tag{30}$$

When E < 1,

$$\frac{x}{S} = 1 - \frac{1}{2}\left(1 + \frac{1}{\sqrt{1 - E^2}}\right)e^{-\left(\frac{2}{E^2T} - \frac{2}{E^2T}\sqrt{1-E^2}\right)t} - \frac{1}{2}\left(1 - \frac{1}{\sqrt{1 - E^2}}\right)e^{-\left(\frac{2}{E^2T} + \frac{2}{E^2T}\sqrt{1-E^2}\right)t} \tag{31}$$

When E > 1,

$$\frac{x}{S} = 1 - \frac{Ee^{-\left(\frac{2t}{E^2T}\right)}}{\sqrt{E^2 - 1}} \left\{ \cos\left[ \left( \frac{2\sqrt{E^2 - 1}}{E^2T} \right) t - \tan^{-1} \frac{1}{\sqrt{E^2 - 1}} \right] \right\} \quad (32)$$

Equations (30), (31), and (32) apply specifically to the acceleration phase of the transient. In this analysis the deceleration phase is approximated by an exponential decay as defined by equation (25). There is, however, very little difference between the values of $\frac{x}{S}$ as defined by equation (30) or equation (31) beyond the inflection point and as defined by the integrated form of equation (25). When $E \leq 1$, the corresponding equations (30) or (31) may therefore be applied in evaluating $\frac{x}{S} = F(t)$ in the deceleration phase of the transient as well as the acceleration phase. When $E > 1$, equation (32), which applies to the acceleration phase, deviates markedly from a first-order response in the deceleration phase. Equation (32) may therefore be applied only up to the inflection point. The time at which the inflection point occurs as evaluated from equation (32) is

$$t_1 = \frac{TE^2}{2\sqrt{E^2 - 1}} \left( \tan^{-1} \sqrt{E^2 - 1} \right) \quad (33)$$

Equation (32) is therefore solved for values of $\frac{x}{S}$ for values of $t$ between zero and $t_1$.

Values of $\frac{x}{S}$ for values of $t > t_1$ are obtained by integrating equation (25) with the initial conditions

$$t = t_1$$

$$x = x_1$$

which yields

$$\frac{x}{S} = 1 - \left(1 - \frac{x_1}{S}\right) e^{-\left(\frac{t - t_1}{T}\right)} \quad (34)$$

The relations defined in this section are summarized in figure 5 along with the expression for $T$ and $E$.

Experimental responses. - As derived in this analysis, the transient response of the servomotor is characterized dynamically by an acceleration phase that is approximately described by a linear second-order differential equation and a deceleration phase that is approximately described by a linear first-order differential equation. The coefficient of the equations for both phases are determined by the two parameters T and E. The parameter T is a function of the motor dimensions and the pressure difference across the motor. The parameter E is a function of the motor dimensions, the load mass (or moment of inertia), and the magnitude of the input step. Figure 6 shows the characteristic agreement between calculated and measured responses in a series of runs in which the factors that determine the parameters T and E have been varied. The data shown were obtained on a rotary servomotor. The servomotor and the experimental procedure are described in appendix A.

In figure 6(a) is shown the agreement between calculated and measured responses at various pressure differences across the motor. This set of runs was made at a fixed step magnitude and a fixed load moment of inertia. Figure 6(b) shows the agreement obtained in a series of runs in which the magnitude of the step was varied while pressure difference and load moment of inertia were held constant. Figure 6(c) shows the agreement obtained in a series of runs made at constant pressure difference and step magnitude in which the load moment of inertia was varied.

As can be seen in figure 6, the calculated responses have provided a close approximation of the actual responses over a very wide range of conditions. It may be of particular interest to note that the effect of the magnitude of the input step predicted by the approximating equations is evident in the measured responses.

## Determination of Peak Cylinder Pressure During Transient Response under an Inertia Load

It has been indicated in the previous section that the pressure difference across the piston during the deceleration phase does not cause the motor response to deviate significantly from a response characterized by an exponential decay. The linear equation (equation (25)) that is therefore adequate to describe the deceleration phase of the position response neglects the variation in deceleration rate and cannot be used to obtain an indication of the peak cylinder pressure during the transient. In the analysis that follows a method will be developed by which an equation similar to equation (16) can be utilized by purely analytical means to determine the peak cylinder pressure that occurs in the deceleration phase.

Initial assumptions. - In the construction of high-speed, high-output hydraulic servomotors, it is usual to employ high supply-pressure differences across the motor. In such instances, the drain pressure $P_d$ is, relative to the supply pressure $P_s$, close to absolute zero. Under this condition, a severe deceleration, resulting from a heavy inertia load, which causes the downstream pressure $P_2$ to rise above $P_s$, will drive the upstream pressure $P_1$ to its limit at essentially absolute zero. In the analysis that follows this condition is assumed to hold. The characteristic pressure variation during such a transient is presented in figure 7.

As shown in figure 7, the pressure transient is divided into three phases. In phases I and III the two pressure curves $(P_1 = F_1(t)$ and $(P_2 = F_2(t))$ are mirror images. In phase II, $P_1$ is considered constant at absolute zero. The calculation of the maximum value of $P_2$ in phase II is based on the determination of the maximum value of deceleration. In order to evaluate the maximum deceleration, it will be necessary to determine the output position and velocity at the beginning of phase II. The symbols to be used in defining the initial conditions for each of the three phases are shown on the upper curve of figure 7.

Determination of initial conditions for phase II. - Up to the inflection point, phase I is identical with the acceleration phase previously treated. It is an assumption that the transients that result in high decelerating pressures will be of the type in which the inertia index $E$ is large; therefore, only the solution to equation (26) for $E > 1$ need be considered. Equation (32) therefore describes the function $x = F(t)$ up to the inflection point. As defined in figure 7, phase I extends beyond the inflection point. The coordinates of the junction of phases I and II are

$$x = x_2$$

$$t = t_2$$

At this point, by definition,

$$P_1 \cong P_d = 0$$

$$P_2 = P_s$$

$$\Delta P_{v,i} = \Delta P_{v,d} = P_s$$

At any point in the transient the piston velocity is related to the flow through the valves by equation (16). Thus, at the junction of phases I and II

$$\dot{x}_2 = \frac{CRW}{A_p}\sqrt{P_s}\,(S - x_2) \tag{35}$$

From equation (8) the following relation may be written:

$$\frac{CRW\sqrt{P_s}}{A_p} = \frac{\sqrt{2}}{T} \tag{36}$$

Substituting equation (36) in equation (35) yields

$$\dot{x}_2 = \sqrt{2}\,\frac{(S - x_2)}{T} \tag{37}$$

From equation (37) it is seen that the velocity at the junction of phases I and II is the velocity corresponding to the inertialess case multiplied by $\sqrt{2}$. At the inflection point the velocity corresponds exactly to the inertialess case. Thus,

$$\dot{x}_1 = \frac{S - x_1}{T}$$

Based on the consideration that

$$(S - x_1) > (S - x_2)$$

the following approximation is made:

$$(S - x_1) \cong \sqrt{2}\,(S - x_2)$$

Hence,

$$\dot{x}_2 \cong \dot{x}_1$$

From this the conclusion is drawn that the piston moves from the inflection point to $x_2$ with substantially the velocity at the inflection point.

The expression for the term $\dot{x}_1$ can be found by differentiating equation (32) and setting $t = t_1$, where $t_1$ is given by equation (33). This yields

$$\dot{x}_2 = \dot{x}_1 = \frac{2Se}{ET} \, -\left(\frac{\tan^{-1}\sqrt{E^2-1}}{\sqrt{E^2-1}}\right) \tag{38}$$

The term $x_2$ is determined by substituting the value of $\dot{x}_2$ (as determined by equation (38) in equation (37)).

Differential equation for phase II of response. - As shown in figure 7, the following relations exist in phase II:

$$P_1 = 0$$

$$\Delta P_p = - P_2$$

$$\Delta P_{v,d} = P_2$$

The pressure drop across the piston is related to the acceleration by the following expression:

$$\Delta P_p = \frac{M\ddot{x}}{A_p}$$

From the condition specified above,

$$\Delta P_{v,d} = - \frac{M}{A_p} \ddot{x}$$

The equation of flow through the valve ports is

$$A_p\dot{x} = \left(CRW\sqrt{- \frac{M}{A_p} \ddot{x}}\right)(S - x)$$

Squaring and rearranging terms gives

$$\left(\frac{A_p{}^3}{C^2R^2W^2M}\right)\left(\frac{\dot{x}}{S - x}\right)^2 + \ddot{x} = 0 \tag{39}$$

From equation (28)

$$\frac{2S}{E^2} = \frac{A_p{}^3}{C^2R^2W^2M}$$

Hence, equation (39) may be written in terms of the inertia index

$$\frac{2}{E^2}\left[\frac{\frac{\dot{x}}{S}}{\left(1 - \frac{x}{S}\right)}\right]^2 + \frac{\ddot{x}}{S} = 0 \tag{40}$$

Determination of maximum value of deceleration. - Differentiating equation (40) and setting $\dddot{x} = 0$ yields

$$\ddot{x}(S - x) + (\dot{x})^2 = 0 \tag{41}$$

Eliminating $\ddot{x}$ between equation (40) and equation (41) gives

$$\frac{2S}{E^2}\frac{(\dot{x})^2}{(S - x)} - (\dot{x})^2 = 0$$

from which

$$\frac{x_m}{S} = 1 - \frac{2}{E^2} \tag{42}$$

Substituting equation (42) in equation (40) yields

$$\ddot{x}_{max} = -\frac{E^2(\dot{x})^2}{2S} \tag{43}$$

The value of $\dot{x}$ at $x = x_m$ is found by integrating equation (40). This integration is shown in appendix B. By inserting this value of $\dot{x}$ in equation (43), the value of $\ddot{x}_{max}$ is obtained. Based on the consideration that $P_1$ equals zero, the relation between the maximum downstream cylinder pressure and the maximum value of the deceleration is

$$P_{2,max} = \frac{M}{A_p}\ddot{x}_{max} \tag{44}$$

It is further shown in appendix B that the ratio $P_{2,max}/P_s$ can be expressed as a function solely of the inertia index. This relation is given below

$$\frac{P_{2,max}}{P_s} = \frac{E^2 e^{2F(E)}}{14.77} \tag{45}$$

where

$$F(E) = \frac{\sqrt{2}}{E} e^{\left(\frac{\tan^{-1}\sqrt{E^2-1}}{\sqrt{E^2-1}}\right)} - \frac{\tan^{-1}\sqrt{E^2-1}}{\sqrt{E^2-1}}$$

It is shown in appendix B that equation (45) has real values for all values of $E > 2.38$.

Comparison of experimental and analytical values of peak cylinder pressure. - Equation (45) is plotted in figure 8 for values of E from 2.38 to 6.5. Also shown in the figure are experimental values obtained on the rotary servomotor described in appendix A. The experimental technique used to obtain the data is also described in appendix A. It can be noted that the experimental values are slightly lower than the analytical curve at low values of E and are in close agreement with the curve at higher values of E. The value of E equal to 5.7, which is the highest experimental value shown, was the highest value that was practicably obtainable with the test equipment. In general, values of E in excess of 6 represent very heavy inertia loads and large step magnitudes.

Effect of high decelerating cylinder pressure on transient response. - In the derivation of the equations that describe the transient response of the servomotor, it was shown that the deceleration phase of the transient response could be approximated by an exponential decay, in which case the variations in the cylinder pressures are neglected. This method of approximation is outlined in figure 5. For transients in which the upstream cylinder pressure is driven to absolute zero, the relations that have been derived for the determination of the peak decelerating cylinder pressure can be used for a more precise determination of the transient response than is afforded by the method of figure 5. The application of these relations to the transient response is presented in appendix B and is outlined in figure 9. A comparison of the method of figure 5 and the method of figure 9 with an experimental response is shown in figure 10. The agreement between the measured response and the response calculated by the method of figure 9 is extremely close. The value of the inertia index in this response was 4.49; hence, from figure 8, the ratio $P_{2,max}/P_s$ equals 1.75. Even with this high decelerating pressure the method of figure 5 provides a fair approximation of the response. The calculations involved in the application of the method outlined in figure 9 are many times longer than that required with the method outlined in figure 5. For this reason the method of figure 9 should be applied only when the need for increased accuracy justifies the longer calculation.

## RESPONSE TO A SINUSOIDAL INPUT

The analysis of the frequency response at no load yields an important parameter used in the analysis of the response under an inertia load. For this reason, both the no-load and the inertia-load cases are treated.

### No-Load Response

Basic character of response. - The basic character of the zero mass response is defined by the linear proportionality between the output velocity and the pilot valve opening (or position error). The proportionality constant between the velocity and the error is the no-load time constant T. For a sinusoidally varying input the instantaneous output velocity is then

$$\dot{x} = \frac{S' \cos \omega t - x}{T} \tag{46}$$

The solution of equation (46) is

$$\frac{x}{S'} = Ae^{i(\omega t+\varphi)} \tag{47}$$

Substituting equation (47) and its derivative in equation (46) gives

$$Ae^{i\varphi} = \frac{1}{1 + i\omega T} \tag{48}$$

The term $Ae^{i\varphi}$ is a vector quantity having an amplitude A and a phase angle $\varphi$. From equation (48)

$$A = \frac{1}{\sqrt{1 + T^2\omega^2}} \tag{49}$$

and

$$\varphi = - \tan^{-1} T\omega \tag{50}$$

For large values of $\omega$

$$A \rightarrow \frac{1}{T\omega}$$

Hence, the asymptote of the response is given by

$$A = \frac{1}{T\omega} \tag{51}$$

The intersection of the asymptotic line and $A = 1$ yields the break frequency and orients the asymptote

$$\omega_1 = \frac{1}{T} \tag{52}$$

Experimental responses. - Figure 11 shows the correlation between the analytical first-order frequency response and the measured frequency response of a servomotor at no load. The servomotor used was the rotary motor described in appendix A. The techniques of instrumentation and experiment are also described in appendix A. The close agreement between the calculated response and the measured response for the wide range of input amplitudes used characterizes the basic linearity of the response of the servomotor at no load.

## Response Under an Inertia Load

It has been shown that under an inertia load the transient response of the servomotor is nonlinear. In the transient response the basic character of the response varied with time. It is therefore to be expected that in the frequency response the basic character of the response will vary with frequency.

Low-frequency amplitude attenuation. - At low frequencies the forces that act on the mass of the system are small and hence the response in this frequency range will be similar to the no-load response. The attenuation may therefore be described by equations (49) and (51). In the log-log plot of amplitude ratio against frequency (fig. 12), an asymptote may then be considered to exist with unity slope and a break frequency of $1/T$. The break frequency of the low-frequency asymptote expressed in cycles per second is

$$f_1 = \frac{1}{2\pi T} \tag{53}$$

High-frequency amplitude attenuation. - At no load the piston velocity is at all times proportional to the valve opening. Therefore, in the response to a sinusoidal input at no load the pilot-valve area is zero at the ends of the output travel (the velocity being zero). Under an inertia load the piston velocity is not proportional to the pilot-valve opening, and hence in the response to a sinusoidal input the valve area is not necessarily zero at the ends of the output travel. If at a given frequency the response of the servomotor is assumed to be essentially sinusoidal, the maximum acceleration can be

considered to occur at the limits of the output travel and hence when the piston velocity is zero. Under the condition of negligible mass of the hydraulic fluid, the pressure difference across the piston at any instant, when the piston velocity is zero and the pilot-valve area is greater than zero, is the pressure difference across the servomotor. Above some frequency the system may then be approximated by a linear system wherein the pressure difference across the piston varies sinusoidally with an amplitude of $(P_s - P_d)$ and with the frequency of the input. On the basis of this approximation the acceleration of the piston is

$$\ddot{x} = \frac{(P_s - P_d)A_p}{M} \sin \omega t \tag{54}$$

Integrating equation (54), introducing the condition that $x$ varies about zero, and neglecting the change in sign yield

$$x = \frac{(P_s - P_d)A_p}{M\omega^2} \sin \omega t \tag{55}$$

After both sides of equation (55) are divided by the output amplitude at zero frequency, the equation relating the amplitude ratio and the frequency is

$$A = \frac{(P_s - P_d)A_p}{S'M\omega^2} \tag{56}$$

In the log-log plot of amplitude ratio against frequency (fig. 12) an asymptote may therefore be considered to exist having a slope of 2 decades per decade. The break frequency of the high-frequency asymptote is found from equation (56) by setting $A = 1$

$$\omega_2 = \sqrt{\frac{(P_s - P_d)A_p}{S'M}} \tag{57}$$

The expression for the value of $\omega_2$ may be made independent of the type of servomotor by relating $\omega_2$ to the no-load time constant and the dimensionless quantity previously defined as the inertia index. The inertia index is defined for the frequency response by replacing the term magnitude of step $S$ with the term amplitude of output sine wave at zero frequency $S'$.

Rewriting equation (28) and introducing the symbol $S'$ in place of $S$ give

$$E' = \frac{\sqrt{2}\ CRW\ \sqrt{MS'}}{A_p^{3/2}}$$

From equation (8)

$$T = \frac{\sqrt{2}\ A_p}{CRW\sqrt{P_s - P_d}}$$

Combining these two relations yields

$$E'T = 2\sqrt{\frac{MS'}{A_p(P_s - P_d)}} \tag{58}$$

Substituting equation (58) in (57) gives

$$\omega_2 = \frac{2}{TE'} \tag{59}$$

The break frequency of the high-frequency asymptote expressed in cycles per second is

$$f_2 = \frac{1}{\pi TE'} \tag{60}$$

The amplitude ratio may also be expressed in terms of T and E'. Substituting equation (58) in equation (56) gives

$$A = \frac{4}{(E')^2T^2\omega^2} \tag{61}$$

Cross-over frequency. - The intersection of the low- and high-frequency asymptotes defines the limit of the low-frequency band and the start of the high-frequency band. For $f_2 > f_1$ this intersection is found by equating the amplitude ratios as defined by equations (51) and (61)

$$\frac{1}{T\omega} = \frac{4}{(E')^2T^2\omega^2}$$

from which

$$\omega_3 = \frac{4}{T(E')^2} \tag{62}$$

The cross-over frequency expressed in cycles per second is

$$f_3 = \frac{2}{\pi T(E')^2} \tag{63}$$

For $f_2 < f_1$ the cross-over frequency occurs at $f_2$; hence

$$f_3 = f_2$$

Correlation of frequency response and transient response. - It has been shown that the derived attenuation asymptotes of the frequency response are functions of the same parameters that govern the derived characteristics of the transient response. It has been shown further that the analytical relation that governs the characteristics in the low-frequency band is the same as the analytical relation that governs the characteristics of the deceleration phase of the transient response (fig. 5). It can also be shown that the linear system used to approximate the acceleration phase of the transient response attenuates along the same asymptote as has been derived for the high-frequency band.

Equation (26) expresses the dynamic equilibrium in the acceleration phase of the response to a step input. Equation (26) rewritten for a sinusoidal input is

$$\frac{T^2(E')^2}{4}\ddot{x} + T\dot{x} + x = S'e^{i\omega t} \tag{64}$$

The solution to equation (64) is

$$\frac{x}{S'} = Ae^{i(\omega t+\varphi)} \tag{65}$$

Substituting equation (65) and its derivatives in equation (64) yields

$$Ae^{i\omega} = \frac{1}{\left(1 - \frac{\omega^2T^2(E')^2}{4}\right) + i\omega T} \tag{66}$$

The term $Ae^{i\omega}$ is a vector quantity having an amplitude $A$ and a phase angle $\varphi$

$$A = \frac{1}{\sqrt{\left(1 - \frac{\omega^2T^2(E')^2}{4}\right)^2 + \omega^2T^2}} \tag{67}$$

$$\varphi = - \tan^{-1} \frac{\omega T}{\left(1 - \frac{\omega^2 T^2 (E')^2}{4}\right)} \tag{68}$$

At high frequencies the relation of equation (67) approaches the asymptote

$$A = \frac{4}{(E')^2 T^2 \omega^2} \tag{69}$$

Equation (69) is identical with equation (61). It is therefore shown that the linear system described by equation (64) attenuates along the same asymptote as the linear system described by equation (26).

Phase shift. - The correlation of the amplitude attenuation with a linear first-order system in the low-frequency band and with a linear second-order system in the high-frequency band provides a basis for the description of the phase shift of the servomotor. The phase shift of linear systems can be represented by straight lines on the coordinates of phase shift against log frequency. The characteristic slope of the straight line for a first-order system is the slope $\frac{d\varphi}{d\omega}$ of the phase-shift-frequency relation at $\varphi = 45^\circ$. The characteristic slope of the straight line for a second-order system is the slope $\frac{d\varphi}{d\omega}$ of the phase-shift-frequency relation at $\varphi = 90^\circ$. The orientation of these lines and the relations for the slopes are shown in figure 12. The derivation of the relations shown in figure 12 is presented in the following paragraphs.

Based on the correlation of the low-frequency-amplitude attenuation with the no-load response, the phase shift is, from equation (50),

$$\varphi = - \tan^{-1} T\omega$$

and, from equation (52), the break frequency in the low-frequency band is

$$\omega_1 = \frac{1}{T}$$

Substituting equation (52) in equation (50) yields

$$\varphi_1 = - \tan^{-1} 1 = 45^\circ$$

Differentiating equation (50) with respect to $\omega$ and setting $\omega = \frac{1}{T}$ yield the slope $\frac{d\varphi}{d\omega}$ at $\alpha = 45^{\circ}$

$$\frac{d\varphi}{d\omega} = \frac{T}{2} \tag{70}$$

The straight line on the semi-log plot may be written

$$\varphi = K \log_{10}\omega \tag{71}$$

Differentiating equation (71) with respect to $\omega$ and solving for K give

$$K = 2.3\omega \frac{d\varphi}{d\omega} \tag{72}$$

Substituting the values of $\frac{d\varphi}{d\omega}$ and $\omega$ at $\varphi = 45^{\circ}$ yields the characteristic slope of the first-order system on the semi-log plot

$$K_1 = 1.15 \tag{73}$$

The phase shift in the low-frequency band may therefore be represented by a straight line on the semi-log plot having a slope of 1.15 radians per decade ($66^{\circ}$/decade) and passing through the point $\omega = \frac{1}{T}$, $\varphi = 45^{\circ}$.

Based on the correlation of the amplitude attenuation in the high-frequency band, with the acceleration phase of the response to a step input, the phase shift in the high-frequency band is characterized by the relation expressed in equation (68). The characteristic slope $\frac{d\varphi}{d\omega}$ of equation (68) is found by differentiating equation (68) and setting $\omega$ equal to $\frac{2}{TE'}$ $(\varphi = 90^{\circ})$

$$\frac{d\varphi}{d\omega} = \frac{T(E')^2}{2} \tag{74}$$

After the substitution of equation (74) and $\omega = \frac{2}{TE'}$ in equation (72), the characteristic slope of the second-order system on the semi-log plot is

$$K_2 = 2.3E' \tag{75}$$

It is a fundamental precept that in representing the response of the servomotor in two frequency bands the relations used to approximate the response shall yield equal amplitude ratios and equal phase shifts at the cross-over frequency. The cross-over frequency has already been defined for equal amplitude ratios. The phase-shift line in the low-frequency band has been previously oriented. The phase-shift line in the high-frequency band therefore intersects the low-frequency phase-shift line at the cross-over frequency and has a slope of $2.3E'$ radians per decade ($132^{\circ}$ E'decade). It should be noted that the low-frequency phase-shift line is limited at $90^{\circ}$ and the high-frequency band phase-shift line is limited at $180^{\circ}$. In figure 12 the cross-over frequency is shown to occur after the low-frequency phase-shift line has reached the $90^{\circ}$ limit. The orientation of the high-frequency phase-shift line for other relative locations of the cross-over frequency is shown in conjunction with the experimental responses.

Experimental responses. - Figure 13 shows the experimentally and analytically determined effect on the frequency response of the hydraulic servomotor of the parameters: load inertia, input amplitude, and pressure. Examples are presented for both the rotary and straight-line types of motor.

In figure 13(a) is shown the effect of load inertia on the amplitude attenuation and on the phase shift of a rotary servomotor. An increase in load inertia results in a reduction in the frequency at which the attenuation becomes rapid. In the analytical expression developed in this paper (summarized in fig. 12) this effect is evident in the increased value of $E'$ with increasing load inertia and the consequent reduction in the values of $f_2$ and $f_3$.

The experimental and calculated frequency response of the same rotary servomotor at various input amplitudes are shown in figure 13(b). The amplitudes given in the figure correspond to the term $\theta'$ and consequently are half the total output stroke at zero frequency. In the case of this particular servomotor, this amplitude corresponds exactly to the amplitude of the input sine wave. The increase in input amplitude is seen to have an effect similar to that of increasing load inertia. This effect is made evident in the analysis by equation (57).

The agreement between experimental and analytical responses for a straight-line servomotor is shown in figures 13(c) and 13(d). Phase shift could not be measured in this installation. Figure 13(c) shows the effect of the pressure difference across the motor. Increased pressure results in increasing the frequency at which the motor begins to attenuate rapidly. In the analytical expressions, the increase in pressure results in a decrease in $T$ and a consequent increase in $f_1$, $f_2$, and $f_3$. The inertia index $E'$ is independent of the pressure

difference and therefore the effect of pressure on $f_2$ and $f_3$ is not as great as the effect on $f_1$. The effect of amplitude shown in figure 13(d) is similar to that already shown in the case of the rotary servomotor in figure 13(b).

In both amplitude attenuation and phase shift the agreement between the measured response and the analytical straight-line approximation is, in general, well within the experimental accuracy. The slopes of the attenuation and phase data clearly demonstrate the first-order characteristics of the response in the low-frequency band and the second-order characteristics of the response in the high-frequency band. The transition from first-order to second-order characteristics at the calculated cross-over frequency is quite pronounced. The values of T and E' shown in figure 13 are based on a value of C of 95.1, on the dimensions of the servomotors as given in appendix A, and on the conditions stated on each plot. In figures 13(c) and 13(d), the pressure differences given are not the actual pressure differences across the motor but are reduced values based on a pressure necessary to overcome friction in the loading carriage. This reduction is discussed in appendix A. In all the other calculated results presented in this paper, no correction whatever was applied to the measured pressure difference across the motor.

## CONCLUDING REMARKS

Application to analysis. - The dynamic relations presented in this paper can be directly applied to the analysis of a given servomotor. The dimensions of the servomotor and the operating pressure difference across the motor determine the no-load time constant T. The inertia index E is then determined from the load inertia and the magnitude or amplitude of the input disturbance. With these two constants determined, the relations for the transient response, the peak cylinder pressure in the transient, and the frequency response can be applied.

The validity of the analysis has been demonstrated by means of recorded transient and frequency responses obtained on two servomotors. In all cases the calculated responses are in close agreement with the measured responses.

Application to design. - The optimum combination of servomotor dimensions to meet specific dynamic requirements involves further discussion of physical considerations that are beyond the scope of this paper. It is nevertheless apparent that, based on this analysis, procedures can be established for the rational design of hydraulic servomotors. In general, the procedures will involve the inversion of the analytical expressions in order that the dimensional parameters (such

as $A_p$, R, and W) may be expressed in terms of the analytical parameters T and E, and the establishment of means of specifying the desired response in terms of the analytical parameters.

Lewis Flight Propulsion Laboratory
National Advisory Committee for Aeronautics
Cleveland, Ohio, May 19, 1952

# APPENDIX A

## APPARATUS AND EXPERIMENTAL PROCEDURES

### Servomotor Dimensions

The two servomotors used in this investigation had the following dimensions:

Straight-line servomotor:

| | |
|---|---|
| Piston area, $A_p$, sq in. | 4.4 |
| Ratio of valve travel to piston travel at fixed input, R, in./in. | 0.1062 |
| Width of valve port, W, in. | 1.33 |

Rotary servomotor:

| | |
|---|---|
| Width of vane, h, in. | 2.000 |
| Inner vane radius, $L_1$, in. | 0.760 |
| Outer vane radius, $L_2$, in. | 2.267 |
| Ratio of valve travel to vane shaft rotation at fixed input, r, in./radians | 0.3125 |
| Width of valve port, W, in. | 0.2225 |

### Transient Response

Position recorder. - Input and output shaft positions were recorded by means of direct-writing oscillographs. The oscillographs were driven by amplifiers. The amplifiers, in turn, received their signal from potentiometers coupled to the servomotor shafts. The frequency response of the amplifier-oscillograph combination was essentially flat over a frequency range from 0 to 80 cycles per second.

Pressure recorder. - Cylinder pressures were also recorded by means of direct-writing oscillographs. The pressure pickups used were of the strain-gage type. The signal developed across the strain-gage bridge was amplified by suitable amplifiers which, in turn, drove the oscillographs. The frequency response of this amplifier-oscillograph combination was essentially flat over a frequency range from 0 to 80 cycles per second. The natural frequency of the pressure pickup was 1000 cycles per second.

Step-input apparatus. - In order to introduce a step change in a mechanical system such as the hydraulic servomotor, it is necessary to

accelerate and decelerate a finite mass (such as the input shaft) at very high rates. The time constant of the servomotor to be tested was about 0.03 second. The very high accelerations that would be required of the input mechanism for the transient to be negligible did not appear to be reasonably attainable in this case. It was therefore decided to use a step input that is obtained by restraining the output. This procedure should be made clear by figure 14.

As can be seen in the photograph, the output shaft is held in position by a wire suitably anchored. The wire used was music wire stressed to approximately 150,000 pounds per square inch. With the output so restrained, the input lever is advanced for the desired magnitude of step. The transient is then triggered by cutting the highly stressed wire. In the transient runs, the output motion was recorded directly. The input motion, which has no meaning in this case, was not recorded. The start of the transient was recorded by placing the restraining wire in the signal circuit of one recorder. A change occurred in the signal voltage when the wire was parted.

The moment of inertia of the load was varied by bolting additional weights to the ends of the bar that was fastened to the output shaft of the servomotor. For the no-load runs a light-weight arm was used in place of the bar that is shown in figure 14.

## Frequency-Response Apparatus

Drive apparatus. - The rotary-servomotor setup for frequency-response measurement is shown in figure 15. In the photograph of figure 15 the servomotor input shaft is on the right-hand side. A rack and gear assembly is coupled to the input shaft. The rack is connected to a variable-stroke crank that is driven by a variable-speed transmission. The drive had a range of from 0.1 to 20 cycles per second.

The straight-line-servomotor setup for frequency-response measurements is shown in figure 16. The input lever is linked directly to a variable-speed, variable-stroke drive. The output potentiometer is coupled to the output shaft by means of a rack and pinion assembly. The servomotor is loaded by means of weights that are bolted to a sliding carriage. Input motion was not measured in this apparatus. The variable speed drive had a range from 0.1 to 11 cycles per second.

Output and phase-angle measurement. - Phase angle was measured only in the case of the rotary servomotor. The circuit diagram showing the method of connecting the potentiometers to the recorder amplifiers is shown in figure 17. By means of the arrangement shown, the output motion and the error between the output and input shaft position are recorded. In the diagram the potentiometers marked input and output

are the two that are visible in figure 15 and are coupled directly to the input and output shaft, respectively. The balance potentiometer is uncoupled.

The output attenuation ratio is obtained directly from the oscillograph traces. The phase angle is obtained by means of the graphical construction shown in figure 18. The input amplitude is laid out to an arbitrary scale. With the use of this scale, the output-amplitude ratio is swung as an arc from the starting point of the input vector. The error-amplitude ratio, referred to amplitude at infinite frequency (obtained by locking output), is swung as an arc from the opposite end of the input vector. The triangle thus formed yields the phase angle.

The particular advantage of this procedure lies in the relatively greater accuracy with which the amplitude of a wave can be measured compared with the determination of the exact point in the cycle at which the maximum height of the wave occurs.

Friction determination. - In the frequency-response runs made with the straight-line servomotor, the limitations imposed by the sinusoidal drive and pumping equipment restricted the range of frequencies to a maximum of 11 cycles per second. In order to obtain a significant range of amplitude ratios below 11 cycles, it was necessary to make these runs at low pressure differences across the motor. The pressure necessary to overcome friction in the servomotor was approximately 2 pounds per square inch and therefore could be neglected in the calculations. The pressure necessary to overcome friction in the loading carriage was as high as 22.5 pounds per square inch at maximum load. This pressure was defined as the pressure necessary to maintain a steady oscillation with a given load on the carriage. The pressure was found to be substantially independent of the frequency in the range of frequency up to 11 cycles per second. The calculated asymptotes shown in figures 13(c) and 13(d) were made with the friction pressure subtracted from the measured pressure difference across the motor.

The procedure previously outlined applies only to figures 13(c) and 13(d). In all the other runs shown, no correction whatever was applied to the measured pressure difference across the motor.

## APPENDIX B

## DERIVATION OF EQUATIONS FOR TRANSIENT RESPONSE IN WHICH UPSTREAM CYLINDER PRESSURE IS LIMITED AT ABSOLUTE ZERO

In the following sections the formal mathematical operations employed in the derivations of the expressions for the peak cylinder pressure and for the position response are presented.

### Peak Cylinder Pressure

Integration of differential equation for limited pressure phase (equation (40)). - The differential equation for the phase of the transient in which the upstream cylinder pressure is limited at absolute zero is, from equation (40),

$$\frac{2S}{E^2}\left(\frac{\dot{x}}{S - x}\right)^2 + \ddot{x} = 0 \tag{B1}$$

The order of the equation may be reduced by means of the following general relation:

$$\ddot{x} = \frac{d(\dot{x})}{dt} \times \frac{dx}{dx} = \dot{x}\,\frac{d(\dot{x})}{dx} \tag{B2}$$

With the substitution of equation (B2) in equation (B1), the reduced equation is obtained

$$\frac{2S}{E^2}\left(\frac{\dot{x}}{S - x}\right)^2 + \dot{x}\,\frac{d(\dot{x})}{dx} = 0$$

Rearranging terms yields

$$\frac{2S}{E^2}\,\frac{dx}{(S - x)^2} + \frac{d(\dot{x})}{\dot{x}} = 0$$

Integrating each term gives

$$\frac{2S}{E^2}\,\frac{1}{(S - x)} + \ln \dot{x} = D \tag{B3}$$

from which

$$\dot{x} = e^{\left(D - \frac{2S}{E^2}\frac{1}{(S-x)}\right)} \tag{B4}$$

With use made of the symbols defined in figure 7, the initial conditions are

$$t = t_2$$

$$x = x_2$$

$$\dot{x} = \dot{x}_2$$

Introducing these values in equation (B3) yields

$$D = \frac{2S}{E^2}\frac{1}{(S - x_2)} + \ln \dot{x}_2 \tag{B5}$$

Relation between ratio of peak pressure to supply pressure and inertia index. - From equation (43)

$$\ddot{x}_{max} = \frac{E^2}{2S}(\dot{x})^2 \tag{B6}$$

From equation (42) the value of $x$ when $\ddot{x}$ is at the maximum value is given by the following relation

$$S - x_m = \frac{2S}{E^2} \tag{B7}$$

With the substitution of equation (B7) into equation (B4), an expression is obtained for the piston velocity when the deceleration is at the maximum value

$$\dot{x}_m = e^{(D-1)} \tag{B8}$$

Substituting equation (B8) in equation (B6) yields

$$\ddot{x}_{max} = \frac{E^2}{2S}\frac{e^{2D}}{e^2} \tag{B9}$$

Based on the consideration that $P_1$ equals zero, the relation between the downstream cylinder pressure $P_2$ and the deceleration is

$$A_p P_2 = M\ddot{x} \tag{B10}$$

Combining equations (B9) and (B10) and dividing by $P_s$ yield

$$\frac{P_{2,max}}{P_s} = \frac{ME^2e^{2D}}{2A_pSe^2P_s} \tag{B11}$$

Based on the consideration that $P_1$ and $P_d$ are zero, the following relation is derived from equation (27):

$$P_s = \frac{4MS}{E^2T^2A_p} \tag{B12}$$

Substituting equation (B12) in the right-hand side of equation (B11) gives

$$\frac{P_{2,max}}{P_s} = \frac{E^4T^2e^{2D}}{8S^2e^2} \tag{B13}$$

Inserting the numerical value of $e^2$ gives

$$\frac{P_{2,max}}{P_s} = \frac{E^4T^2e^{2D}}{59.1S^2} \tag{B14}$$

The exponent D may be expressed in terms of the relations that have been derived for $x_2$ and $\dot{x}_2$. From equation (37)

$$S - x_2 = \frac{T\dot{x}_2}{\sqrt{2}} \tag{B15}$$

and from equation (38)

$$\dot{x}_2 = \frac{2Se}{TK}^{-\left(\frac{\tan^{-1} K}{K}\right)} \sin(\tan^{-1} K) \tag{B16}$$

where $K = \sqrt{E^2 - 1}$

By use of the trigonometric identity

$$\sin a = \frac{\tan a}{\sqrt{1 + \tan^2 a}}$$

it can be shown that

$$\sin\left(\tan^{-1} K\right) = \frac{K}{\sqrt{1 + K^2}}$$

Furthermore,

$$\sqrt{1 + K^2} = E$$

Hence,

$$\sin\left(\tan^{-1} K\right) = \frac{K}{E}$$

and equation (B16) may be written

$$\dot{x}_2 = \frac{2Se}{TE}^{-\left(\frac{\tan^{-1} K}{K}\right)} \tag{B17}$$

Substituting equation (B17) in equation (B15) yields

$$(S - x_2) = \frac{\sqrt{2}Se}{E}^{-\left(\frac{\tan^{-1} K}{K}\right)} \tag{B18}$$

Substituting equations (B17) and (B18) in equation (B5) gives

$$D = \frac{\sqrt{2}}{E} e^{\left(\frac{\tan^{-1} K}{K}\right)} - \frac{\tan^{-1} K}{K} + \ln \frac{2S}{TE} \tag{B19}$$

Let

$$\frac{\sqrt{2}}{E} e^{\left(\frac{\tan^{-1} K}{K}\right)} - \frac{\tan^{-1} K}{K} = F(E)$$

Then

$$D = F(E) + \ln \frac{2S}{TE}$$

and

$$e^{2D} = \frac{4S^2}{T^2E^2} e^{\left[2F(E)\right]} \tag{B20}$$

Substituting equation (B20) in equation (B14) gives

$$\frac{P_{2,max}}{P_s} = \frac{E^2 e}{14.77}\left[2F(E)\right] \tag{B21}$$

It can be seen from figure 7 that equation (B21) will yield real values only if the following relation exists:

$$\frac{x_m}{S} > \frac{x_2}{S}$$

Because $x_m/S$ and $x_2/S$ are both functions solely of E, the value of E when $x_m/S = x_2/S$ represents the limiting value of E for real values of $P_{2,max}/P_s$.

From equation (B7)

$$\frac{x_m}{S} = 1 - \frac{2}{E^2} \tag{B22}$$

From equation (B18)

$$\frac{x_2}{S} = 1 - \frac{\sqrt{2}e}{E}^{-\left(\frac{\tan^{-1}\sqrt{E^2-1}}{\sqrt{E^2-1}}\right)} \tag{B23}$$

Equating equations (B7) and (B18) gives

$$E = \sqrt{2}e^{\left(\frac{\tan^{-1}\sqrt{E^2-1}}{\sqrt{E^2-1}}\right)} \tag{B24}$$

The value of E that satisfies this relation is 2.38.

Because $x_m/S$ approaches unity more rapidly than $x_2/S$ as E increases, $P_{2,max}/P_s$ as defined by equation (B21) has real values for $E > 2.38$. The validity of this proof is demonstrated by the evaluation of equation (B21) at $E = 2.38$. Inserting this value of E in equation (B21) yields

$$\frac{P_{2,max}}{P_s} = 1$$

Position Response

Determination of initial coordinates of phase II. - From equation (37)

$$\frac{x_2}{S} = 1 - \frac{T}{\sqrt{2}} \frac{\dot{x}_2}{S} \tag{B25}$$

From equation (38)

$$\frac{\dot{x}_2}{S} = \frac{2}{ET} e^{-\left(\frac{\tan^{-1}\sqrt{E^2-1}}{\sqrt{E^2-1}}\right)} \tag{B26}$$

Substituting equation (B26) in equation (B25) yields

$$\frac{x_2}{S} = 1 - \frac{\sqrt{2}}{E} e^{-\left(\frac{\tan^{-1}\sqrt{E^2-1}}{\sqrt{E^2-1}}\right)} \tag{B27}$$

The velocity is constant from the point $\frac{x_1}{S}$ to the point $\frac{x_2}{S}$; hence,

$$t_2 = t_1 + \left(\frac{\frac{x_2}{S} - \frac{x_1}{S}}{\frac{\dot{x}}{S}}\right) \tag{B29}$$

Integration of differential equation for phase II. - The first step in this integration is presented in the previous section in which equation (B1) is integrated to $\dot{x}$ (equation (B4)).

Let

$$\frac{2S}{E^2} \frac{1}{(S - x)} = u$$

$$du = \frac{2S}{E^2} (S - x)^{-2} \, dx$$

$$dx = \frac{2S}{E^2} \times \frac{1}{u^2} \, du$$

Making these substitutions in equation (B4) and rearranging terms yield

$$dt = \left(\frac{2Se^{-D}}{E^2}\right)\frac{e^u}{u^2}\,du \tag{B30}$$

$$\int \frac{e^u}{u^2}\,du = \ln u - \frac{e^u}{u} + \sum_{n=1}^{n=\infty} \frac{u^n}{n \times n!} \tag{B31}$$

The integrated equation is then

$$t = \left(\frac{2Se^{-D}}{E^2}\right)\left(\ln u - \frac{e^u}{u} + \sum_{n=1}^{n=\infty} \frac{u^n}{n \times n!} + H\right) \tag{B32}$$

The constant H is evaluated by introducing the initial condition

$$t = t_2$$

$$x = x_2$$

Hence,

$$H = t_2 - \frac{2S}{E^2}\,e^{-D}\left\{\ln z - \frac{e^z}{z} + \sum_{n=1}^{n=\infty} \frac{z^n}{n \times n!}\right\} \tag{B33}$$

where

$$z = \frac{2S}{E^2}\,\frac{1}{(S - x_2)}$$

Determination of initial conditions for phase III (fig. 7). - As defined in figure 7, the coordinates of the junction of phases II and III are

$$x = x_3$$

$$t = t_3$$

As further defined, the following conditions exist at $t = t_3$:

$$P_1 = P_2 \cong 0$$

$$P_2 = P_s$$

$$\Delta P_p = - P_s$$

$$\Delta P_{v,i} = \Delta P_{v,d} = P_s$$

Hence,

$$\ddot{x}_3 = - \frac{A_p P_s}{M}$$

By equation (7)

$$\dot{x}_3 = \frac{CRW}{A_p} \sqrt{P_s} \, (S - x_3) \tag{B34}$$

Substituting equation (36) yields

$$\dot{x}_3 = \frac{\sqrt{2}}{T} \, (S - x_3) \tag{B35}$$

From equation (B4) a second velocity-position relation is obtained

$$\dot{x}_3 = e^{\left( D - \frac{2S}{E^2} \frac{1}{(S - x_3)} \right)} \tag{B36}$$

Combining equations (B35) and (B36) yields

$$D = \frac{2S}{E^2} \frac{1}{(S - x_3)} + \ln \frac{\sqrt{2}}{T} \, (S - x_3) \tag{B37}$$

The constant D is evaluated by means of equation (B19) and $x_3$ is determined graphically from equation (B37). The coordinate $t_3$ is evaluated by means of $x_3$ and equation (B32).

Equation for phase III of response. - Phase III is identical with the deceleration phase of figure 3. Therefore, following the derivation of equation (34), the equation of the response in phase III is

$$\frac{x}{S} = 1 - \left( 1 - \frac{x_3}{S} \right) e^{-\left( \frac{t - t_3}{T} \right)} \tag{B38}$$

## REFERENCE

1. Grosser, Christian E.: Valve-Controlled Servomechanisms. Applied Hydraulics, vol. 1, no. 7, Aug. 1948, pp. 15-19.

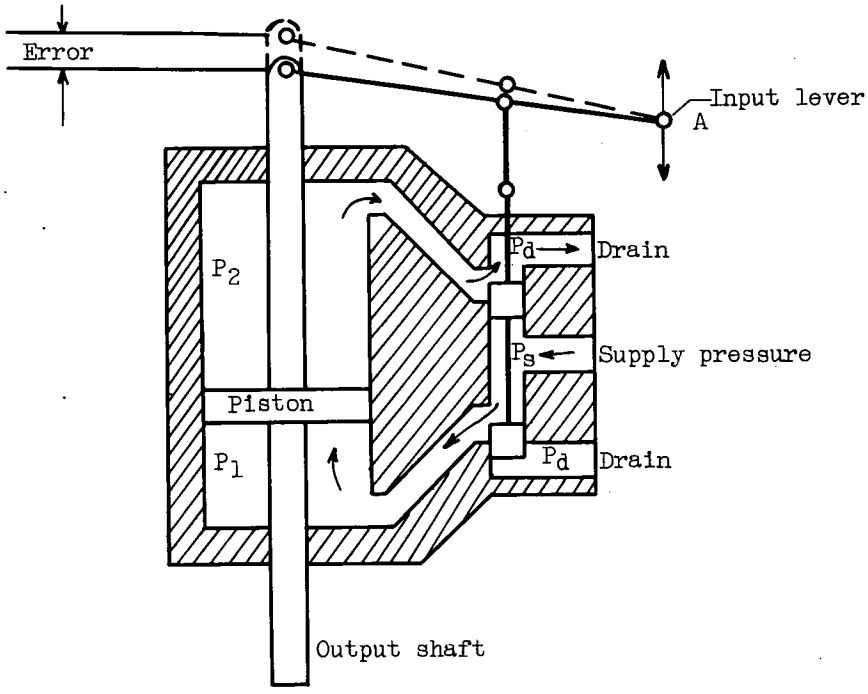


(a) Straight-line servomotor.

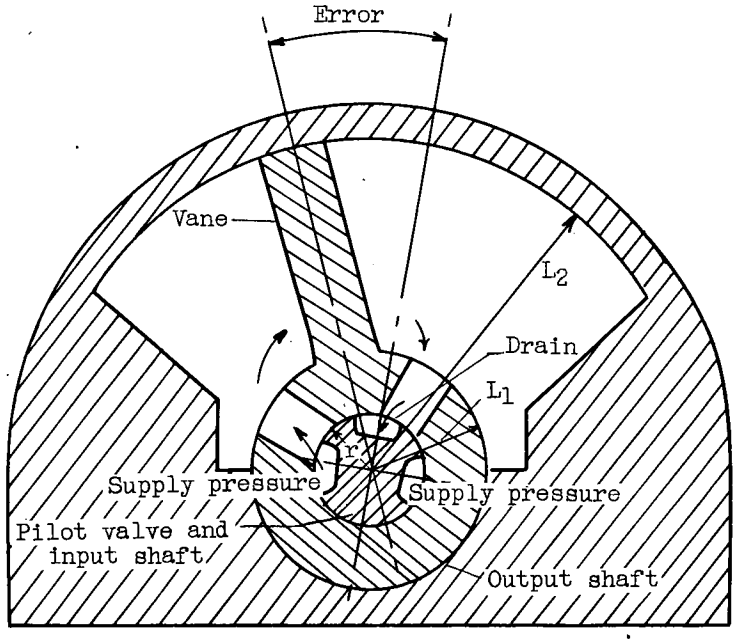


(b) Rotary servomotor.

Figure 1. - Schematic drawings of two types of hydraulic servomotors with mechanical feedback.

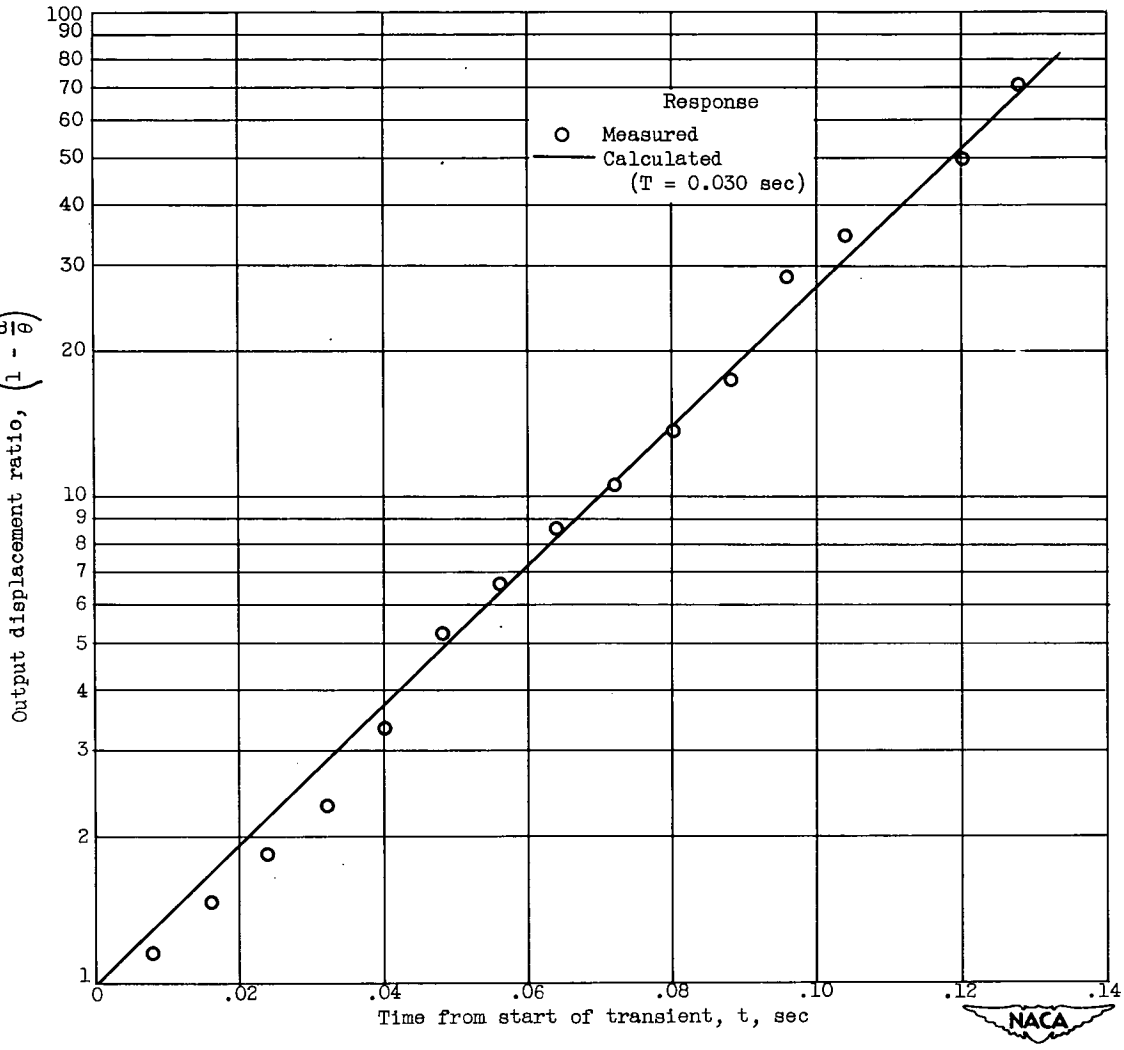


Figure 2. - Response of a hydraulic servomotor to a step input under negligible inertia load. Rotary servomotor; torque-inertia ratio, 3,500,000 radians per second per second; supply pressure, 1000 pounds per square inch; total shaft displacement, 20°.

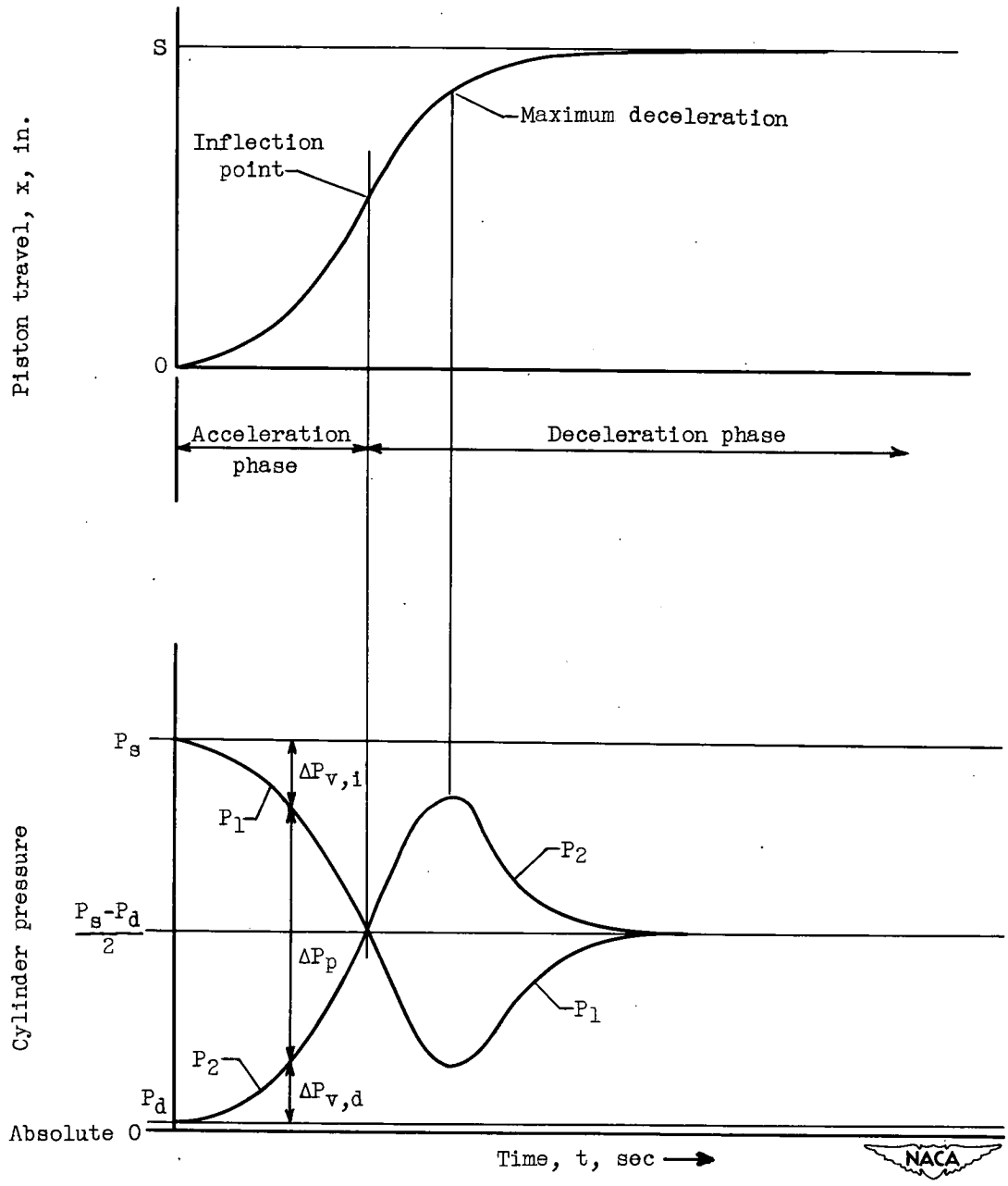


Figure 3. - Characteristic pressure variations during transient response of a hydraulic servomotor with mechanical feedback. Step input and inertia load (cylinder pressures not limited).

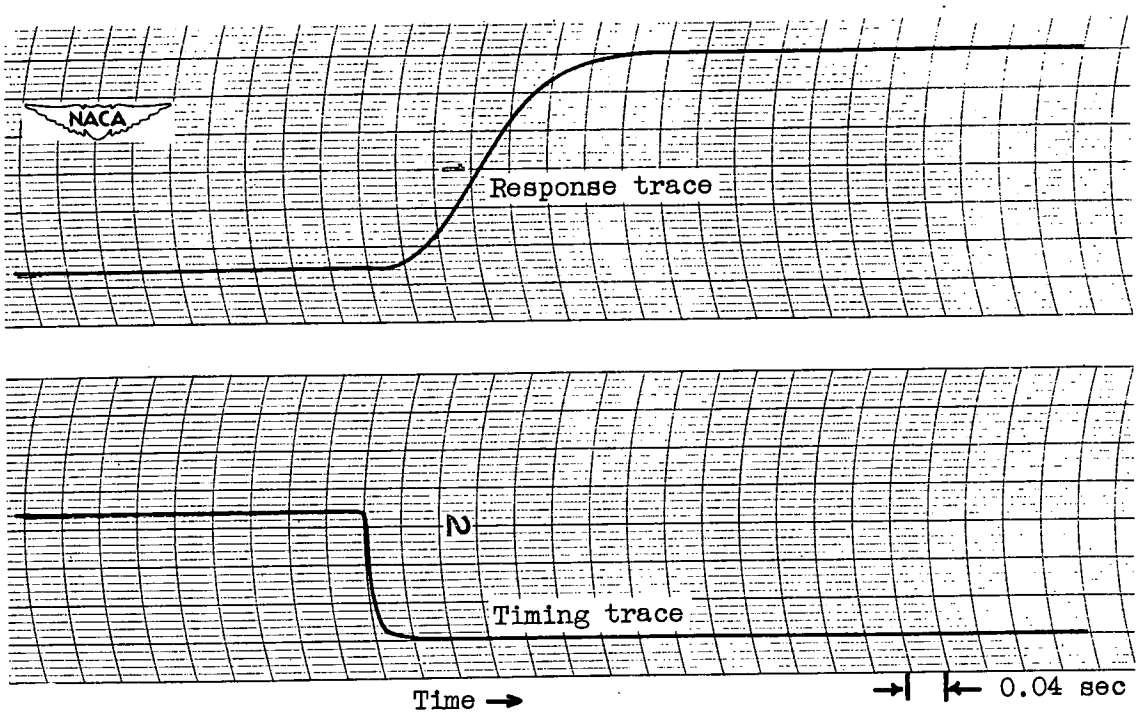


Figure 4. - Oscillographic record of response to a step input of a hydraulic servomotor under an inertia load.

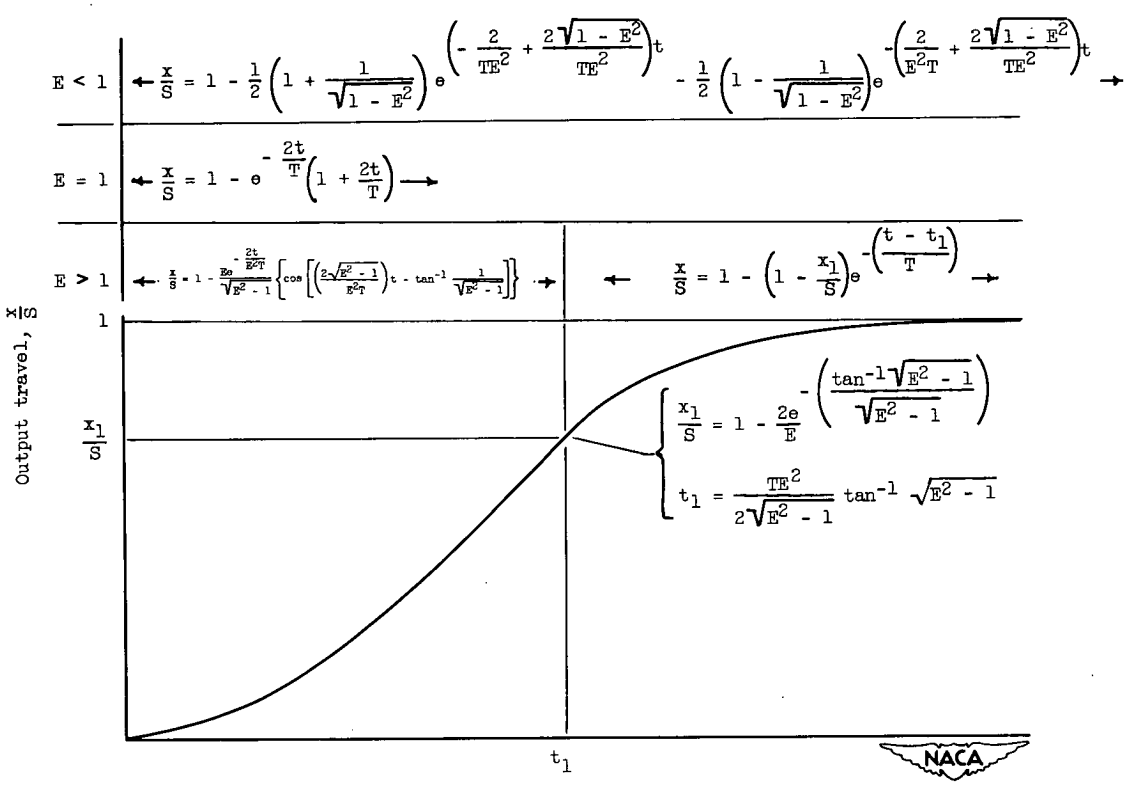


Straight-line servomotor

$$T = \frac{\sqrt{2}A_p}{CRW\sqrt{P_s - P_d}}$$

$$E = \frac{\sqrt{2}CRW\sqrt{MS}}{A_p^{3/2}}$$

Rotary servomotor

$$T = \frac{h\left(L_2^2 - L_1^2\right)}{\sqrt{2}CrW\sqrt{P_s - P_d}}$$

$$E = \frac{4CrW\sqrt{\theta J}}{\left[h\left(L_2^2 - L_1^2\right)\right]^{3/2}}$$

Figure 5. - Summary of linear relations for transient response of hydraulic servomotors with mechanical feedback.

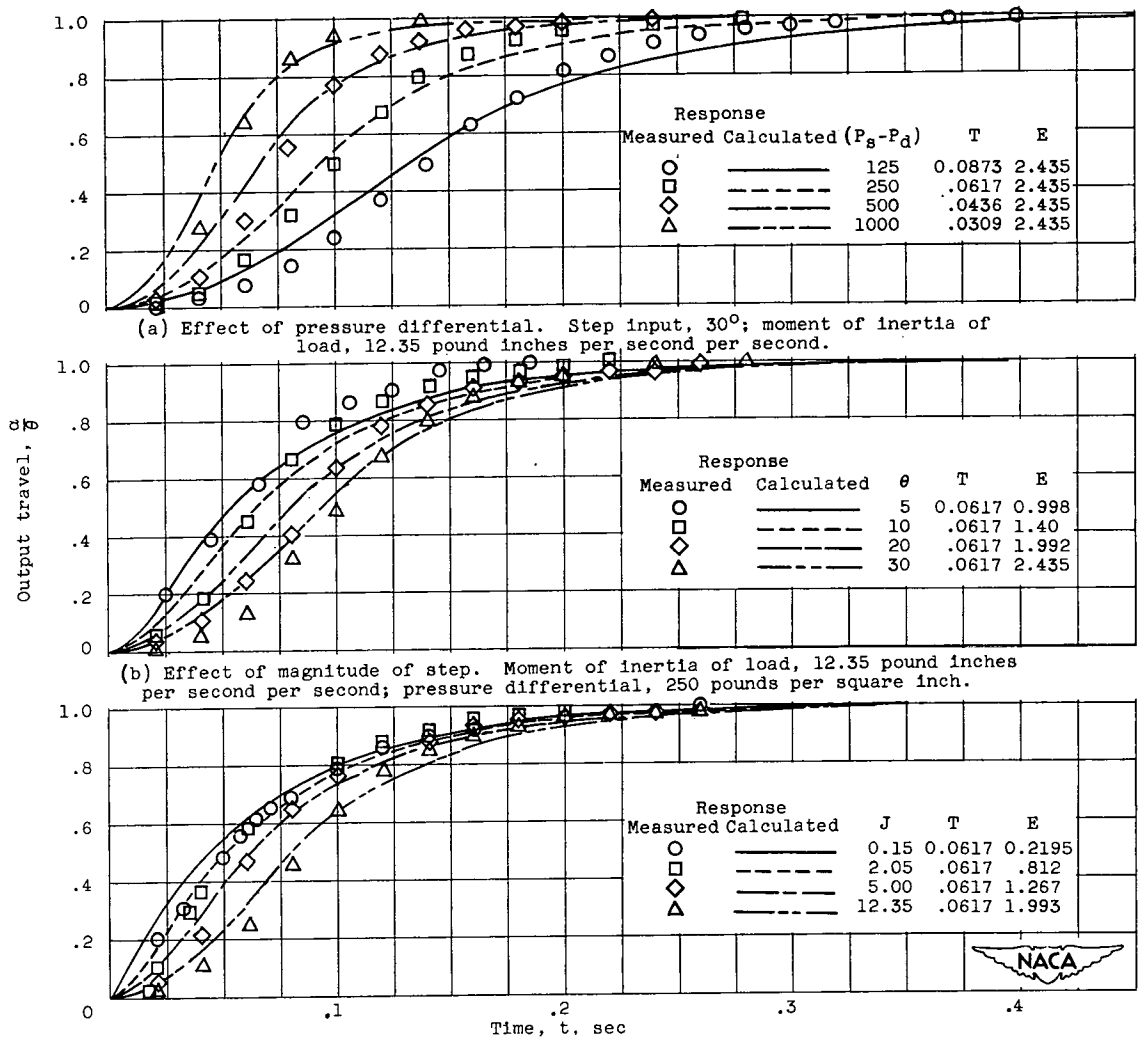


(a) Effect of pressure differential. Step input, 30°; moment of inertia of load, 12.35 pound inches per second per second.

(b) Effect of magnitude of step. Moment of inertia of load, 12.35 pound inches per second per second; pressure differential, 250 pounds per square inch.

(c) Effect of load inertia. Step input, 20°; pressure differential, 250 pounds per square inch.

Figure 6. - Responses of a hydraulic servomotor to a step input under inertia load. Rotary servomotor.

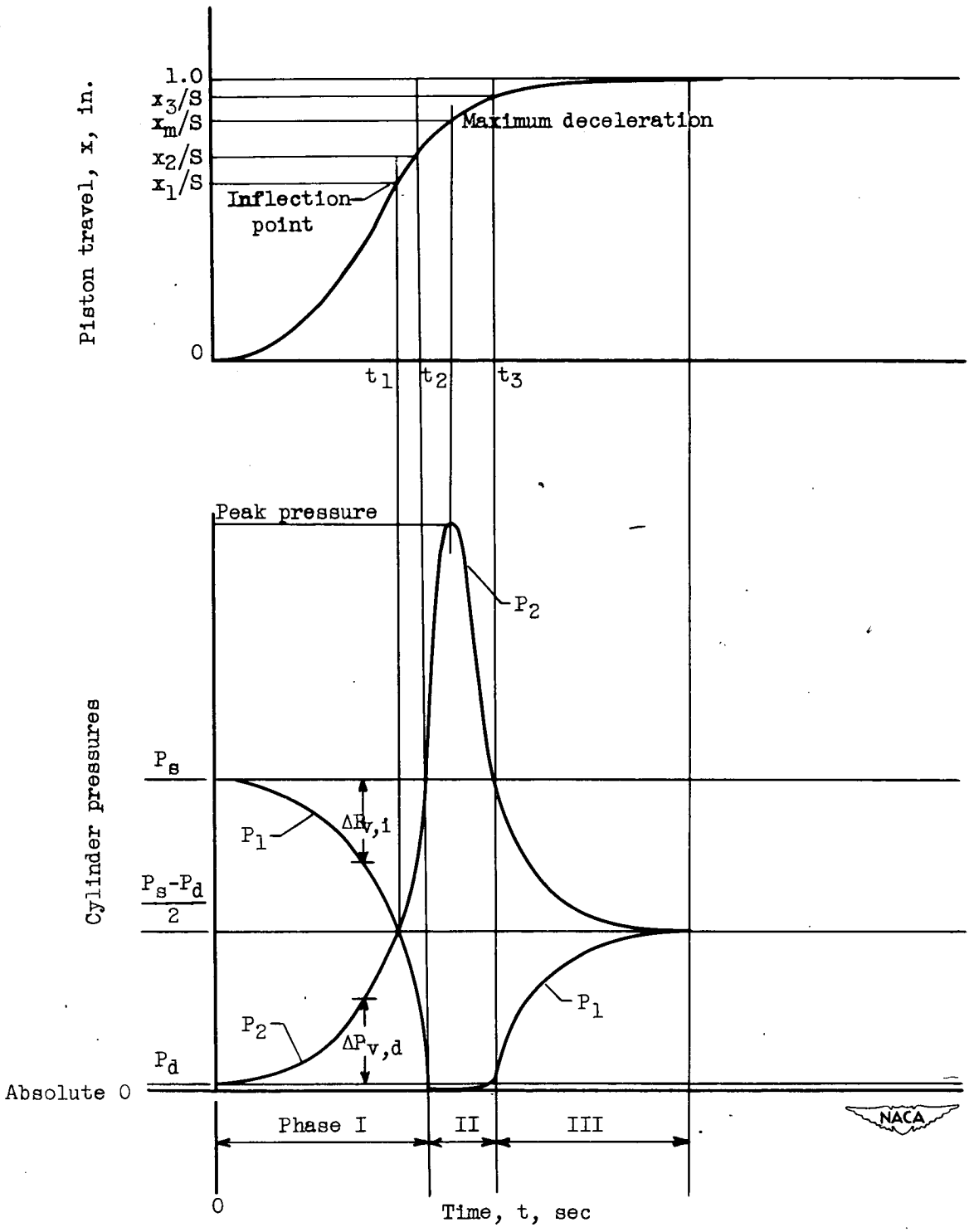


Figure 7. - Characteristic pressure variations during transient response of a hydraulic servomotor with mechanical feedback. Step input and inertia load (upstream cylinder pressure limited at absolute zero).

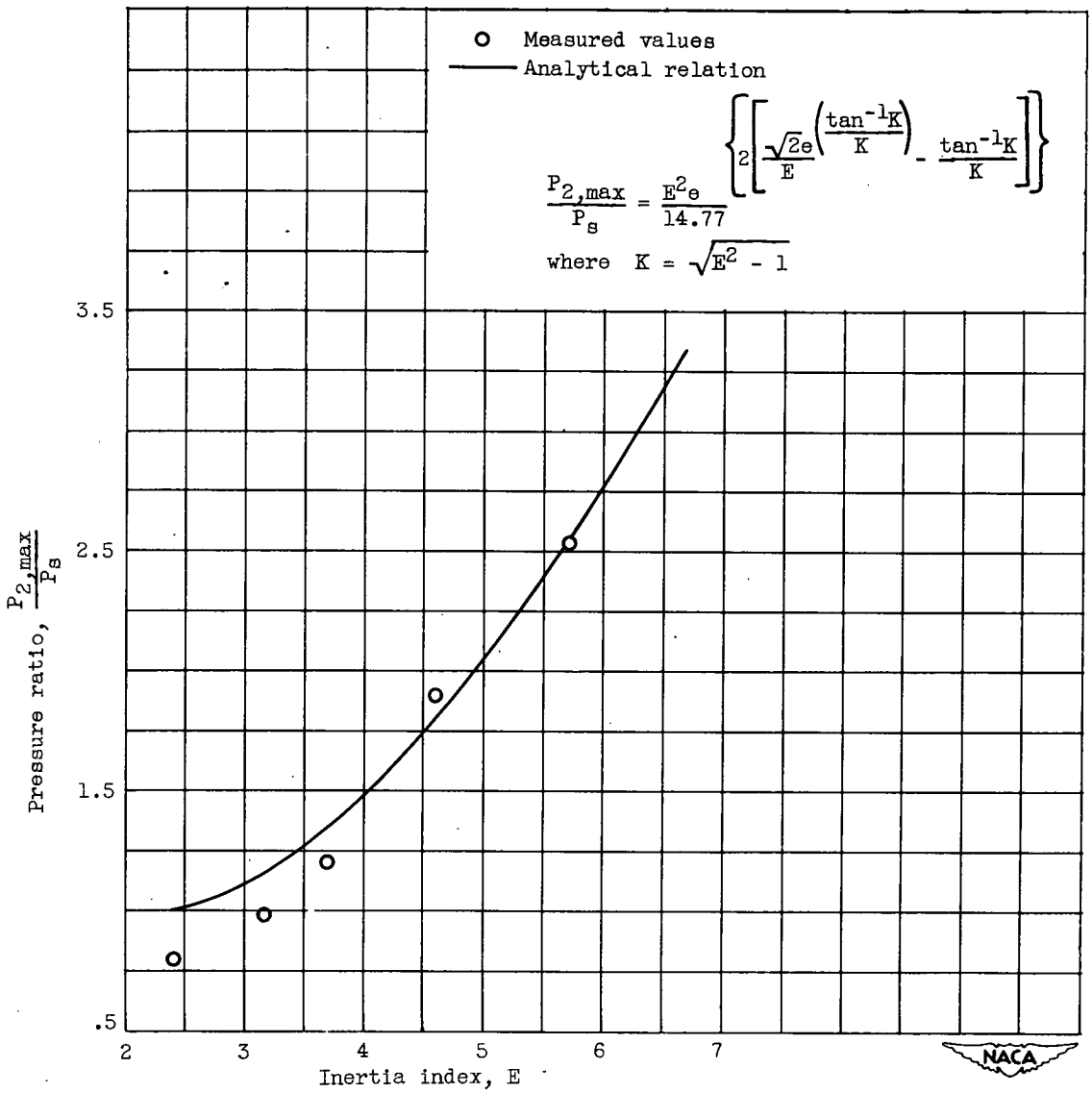


Figure 8. - Ratio of peak transient cylinder pressure to supply pressure as a function of inertia index. Hydraulic servomotor with mechanical feedback.

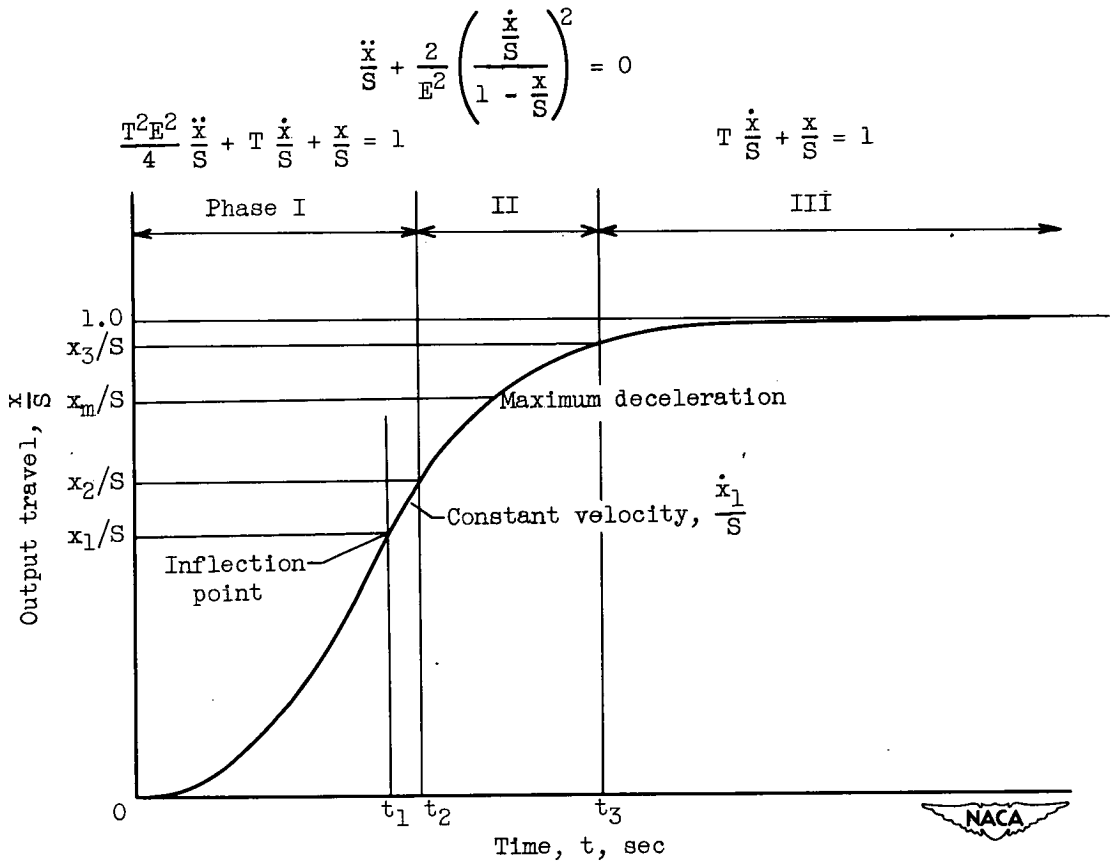


Figure 9. - Analytical relations for approximating transient response of a hydraulic servomotor with mechanical feedback. Step input and inertia load (upstream cylinder pressure limited at absolute zero).

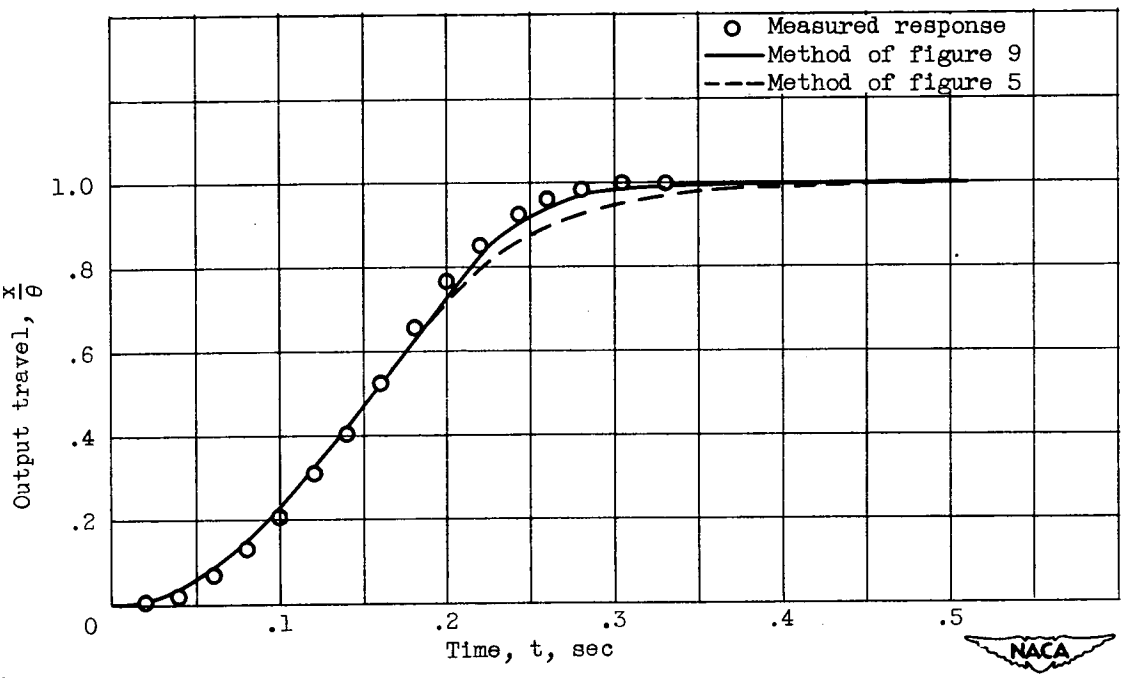


Figure 10. - Comparison of method of figures 5 and 9 with a measured response. Transient response of a hydraulic servomotor with mechanical feedback. Rotary servomotor; step input, 30°; moment of inertia of load, 41.75 pound inches per second per second; pressure differential, 250 pounds per square inch. Inertia index, E, 4.49; no-load time constant, T, 0.0617 second.

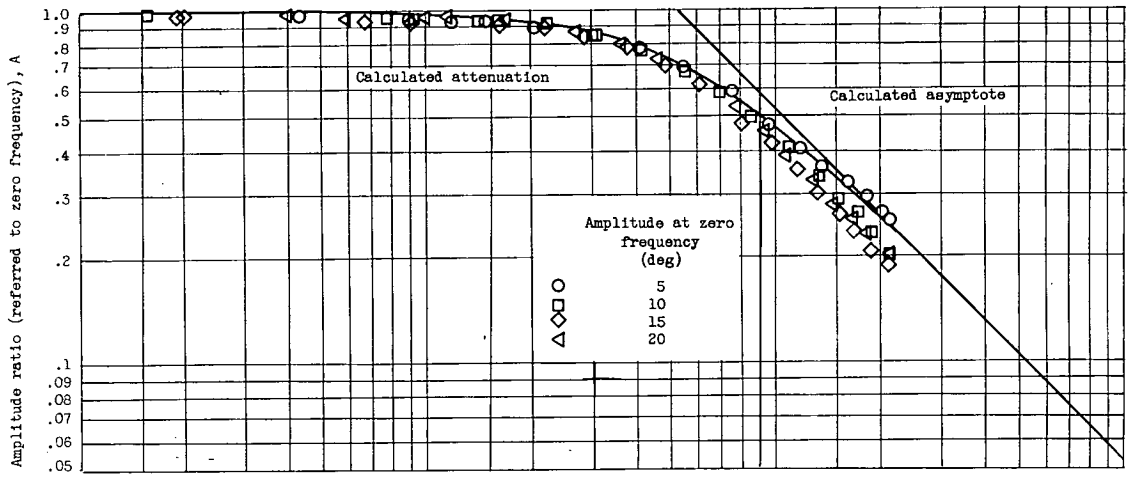


(a) Amplitude attenuation.

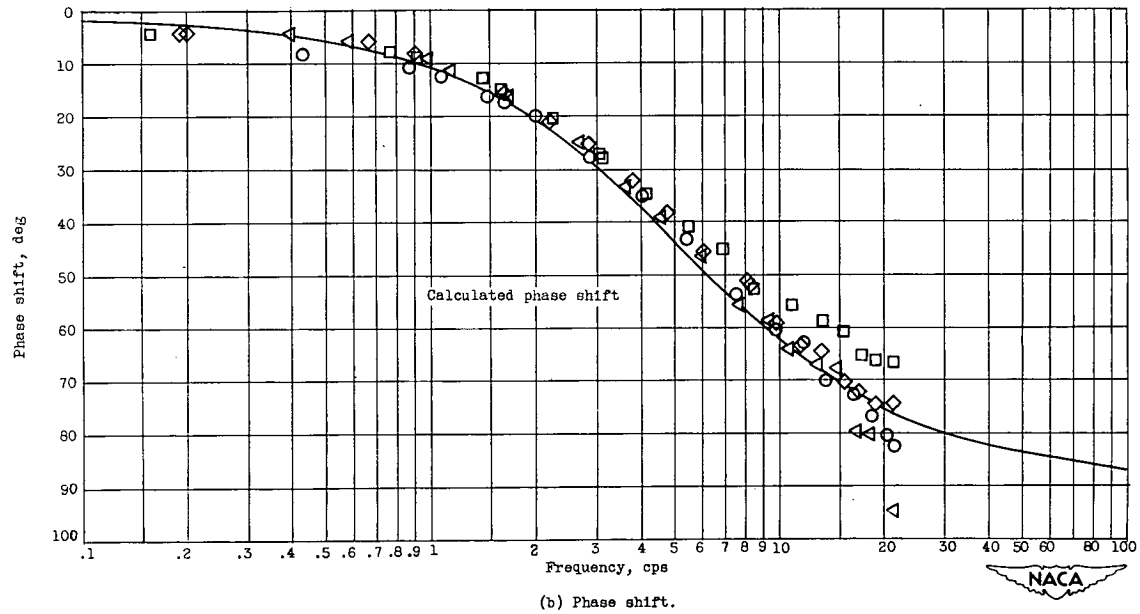


(b) Phase shift.

Figure 11. - Frequency response of a hydraulic servomotor under negligible inertia load. Rotary servomotor; torque-inertia ratio, 3,500,000 radians per second per second; supply pressure, 1000 pounds per square inch.

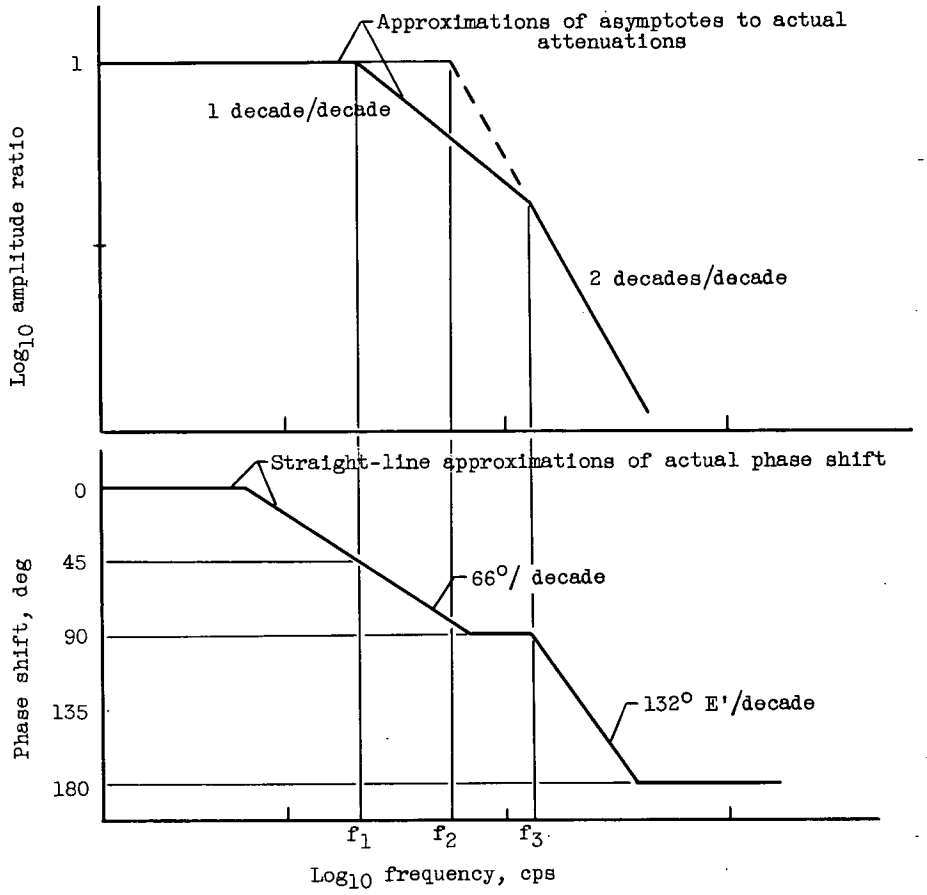


$$f_1 = \frac{1}{2\pi T}$$

$$f_2 = \frac{1}{\pi T E'}$$

$$f_3 = \frac{2}{\pi T (E')^2}$$

Straight-line servomotor

$$T = \frac{A_p\sqrt{2}}{CRW\sqrt{P_s - P_d}}$$

$$E' = \frac{\sqrt{2}CRW\sqrt{MS'}}{A_p^{3/2}}$$

Rotary servomotor

$$T = \frac{h\left(L_2^2 - L_1^2\right)}{\sqrt{2}CrW\sqrt{P_s - P_d}}$$

$$E' = \frac{4CrW\sqrt{\theta' J}}{\left[h\left(L_2^2 - L_1^2\right)\right]^{3/2}}$$

Figure 12. - Summary of linear relations for frequency response of hydraulic servomotors with mechanical feedback.

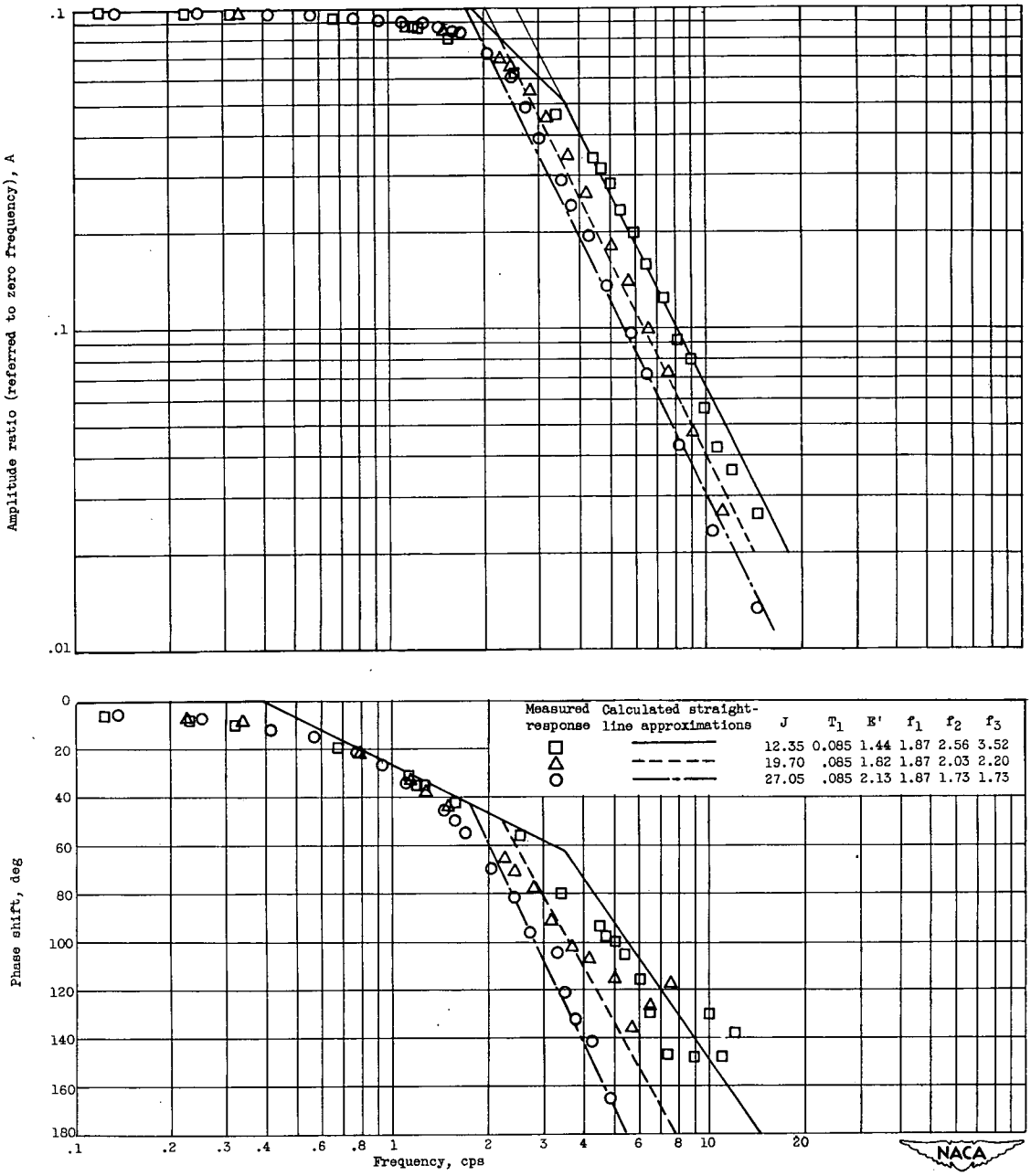


(a) Effect of load inertia J. Rotary servomotor; amplitude at zero frequency, 10°; pressure differential, 125 pounds per square inch.

Figure 13. - Frequency responses of hydraulic servomotors under inertia load.

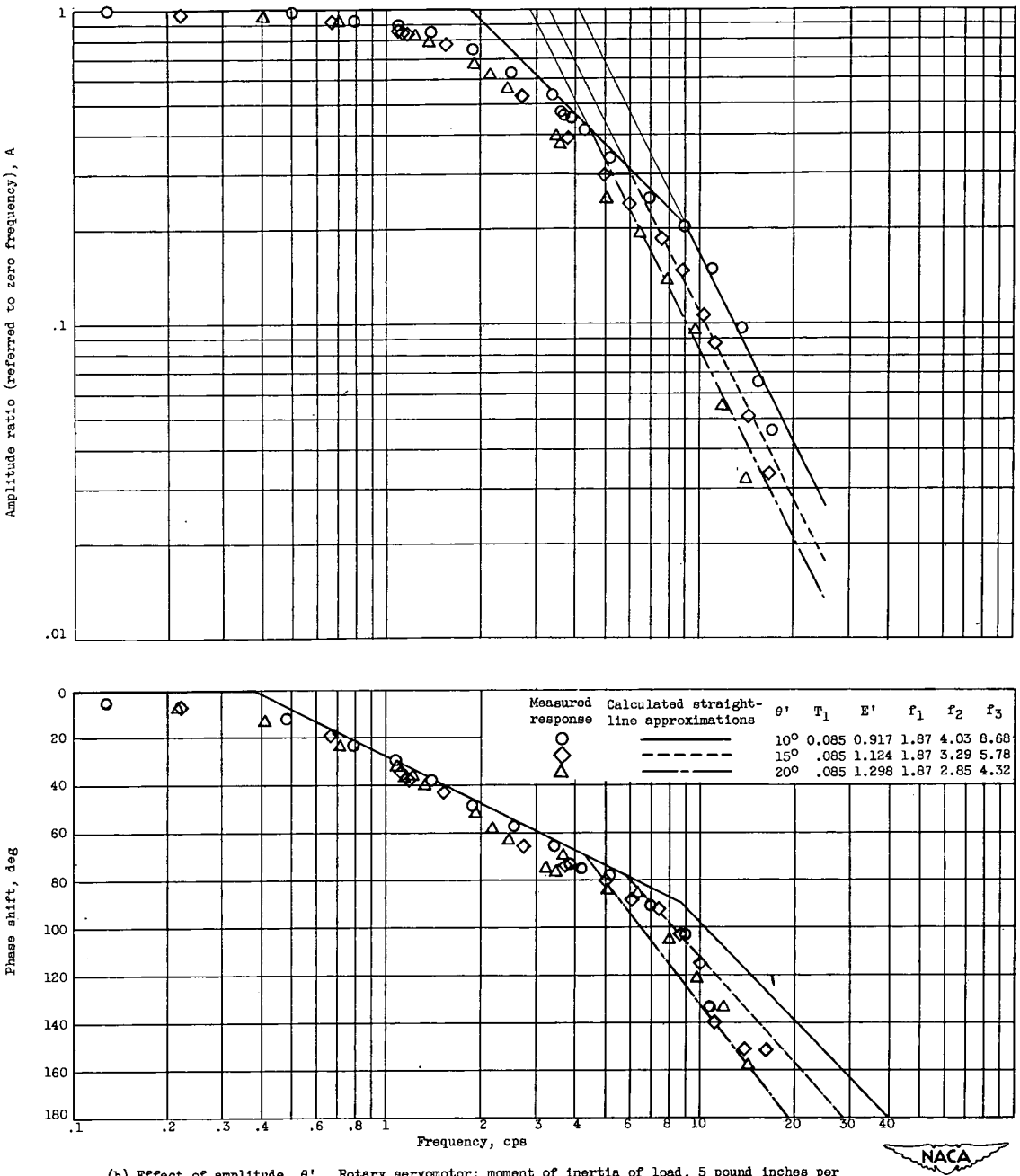


(b) Effect of amplitude $\theta'$. Rotary servomotor; moment of inertia of load, 5 pound inches per second per second; pressure differential, 125 pounds per square inch.

Figure 13. - Continued. Frequency responses of hydraulic servomotors under inertia load.

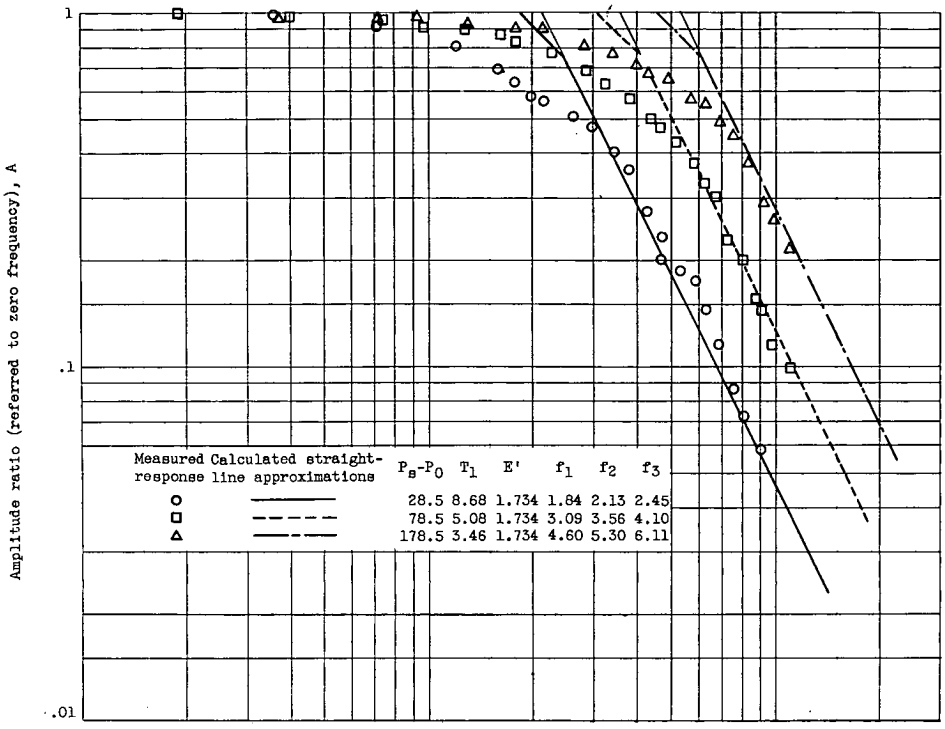


(c) Effect of pressure differential $P_s-P_d$. Straight-line servomotor; load mass, 1.08 pounds per second per second per inch; amplitude at zero frequency, 0.65 inch.

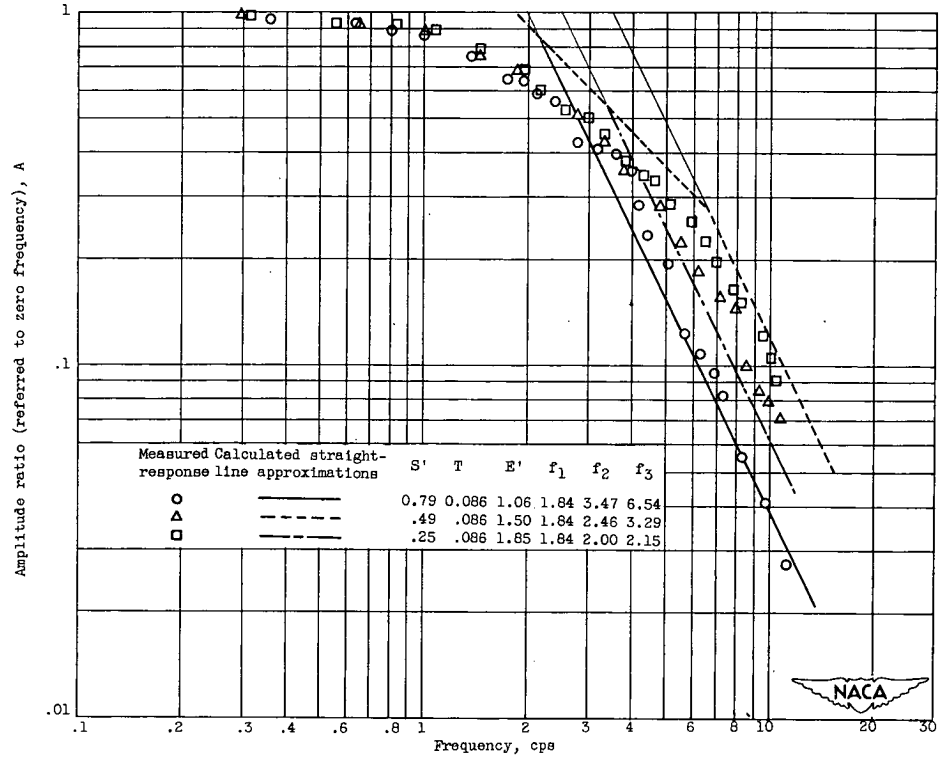


(d) Effect of amplitude S'. Straight-line servomotor; load mass, 1.08 pounds per second per second per inch; pressure differential, 28.5 pounds per square inch.

Figure 13. - Concluded. Frequency responses of hydraulic servomotors under inertia load.

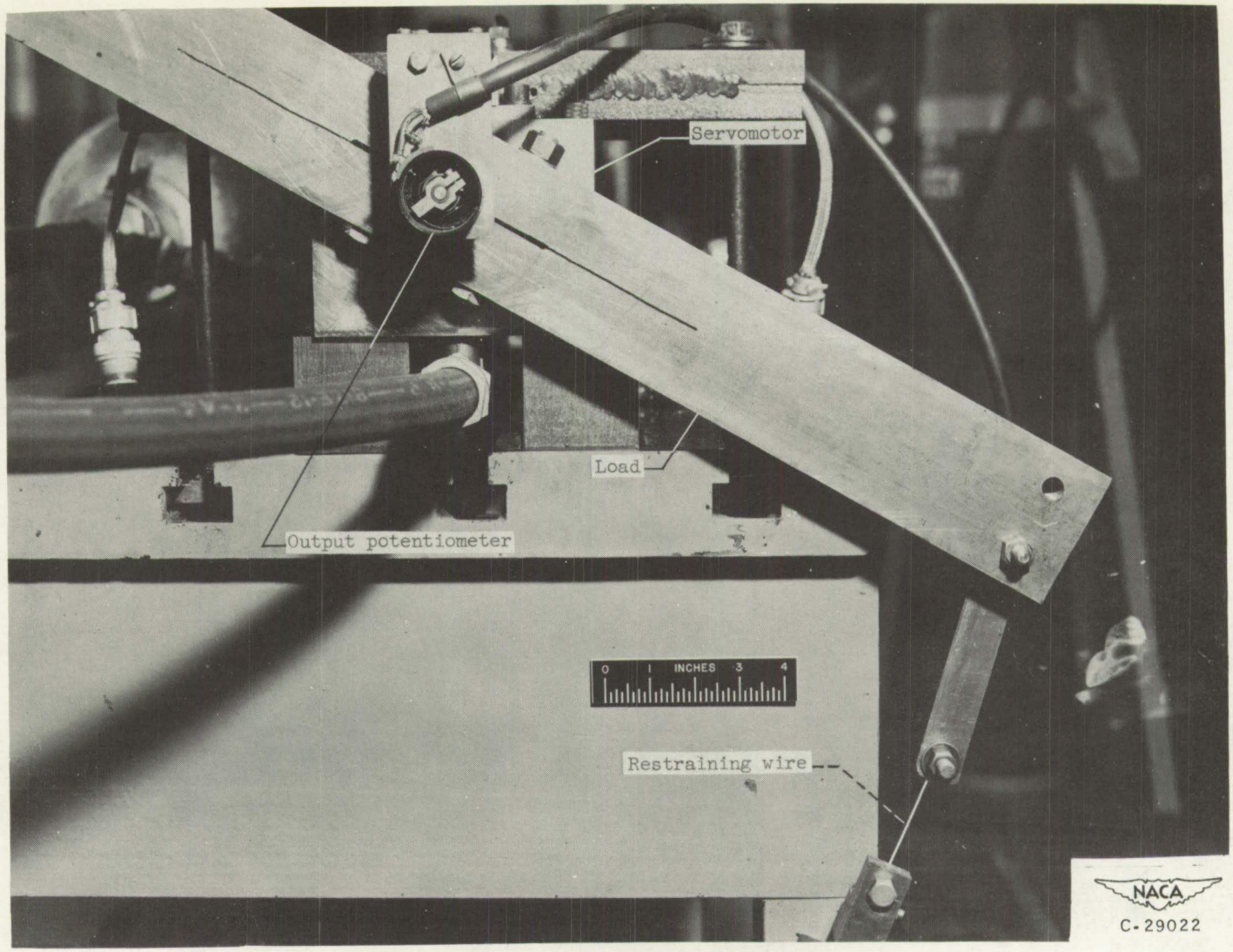


Figure 14. - Rotary hydraulic servomotor instrumented for recording transient response to a step input.

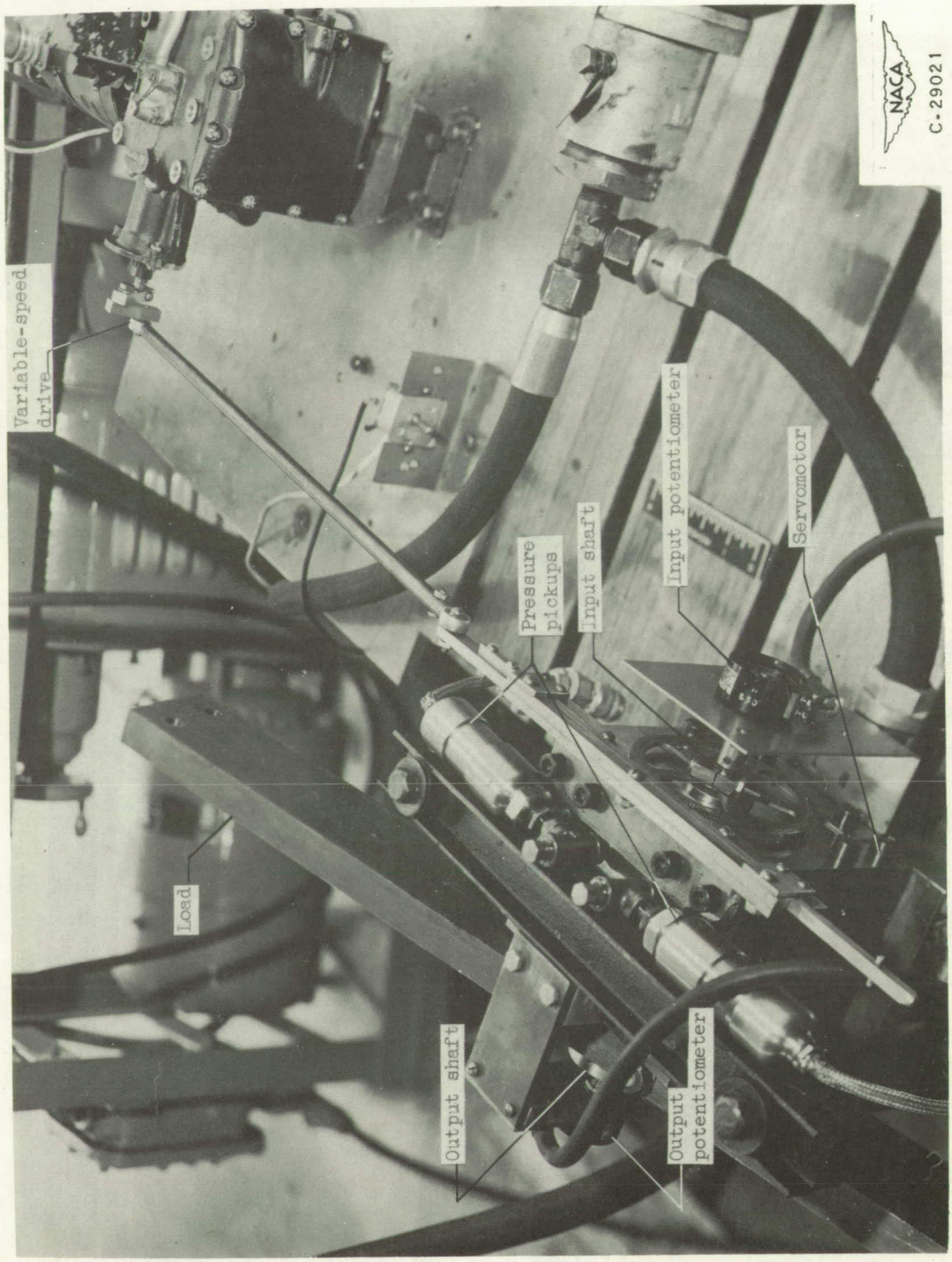


Figure 15. - Rotary hydraulic servomotor instrumented for recording response to a sinusoidally varying input.

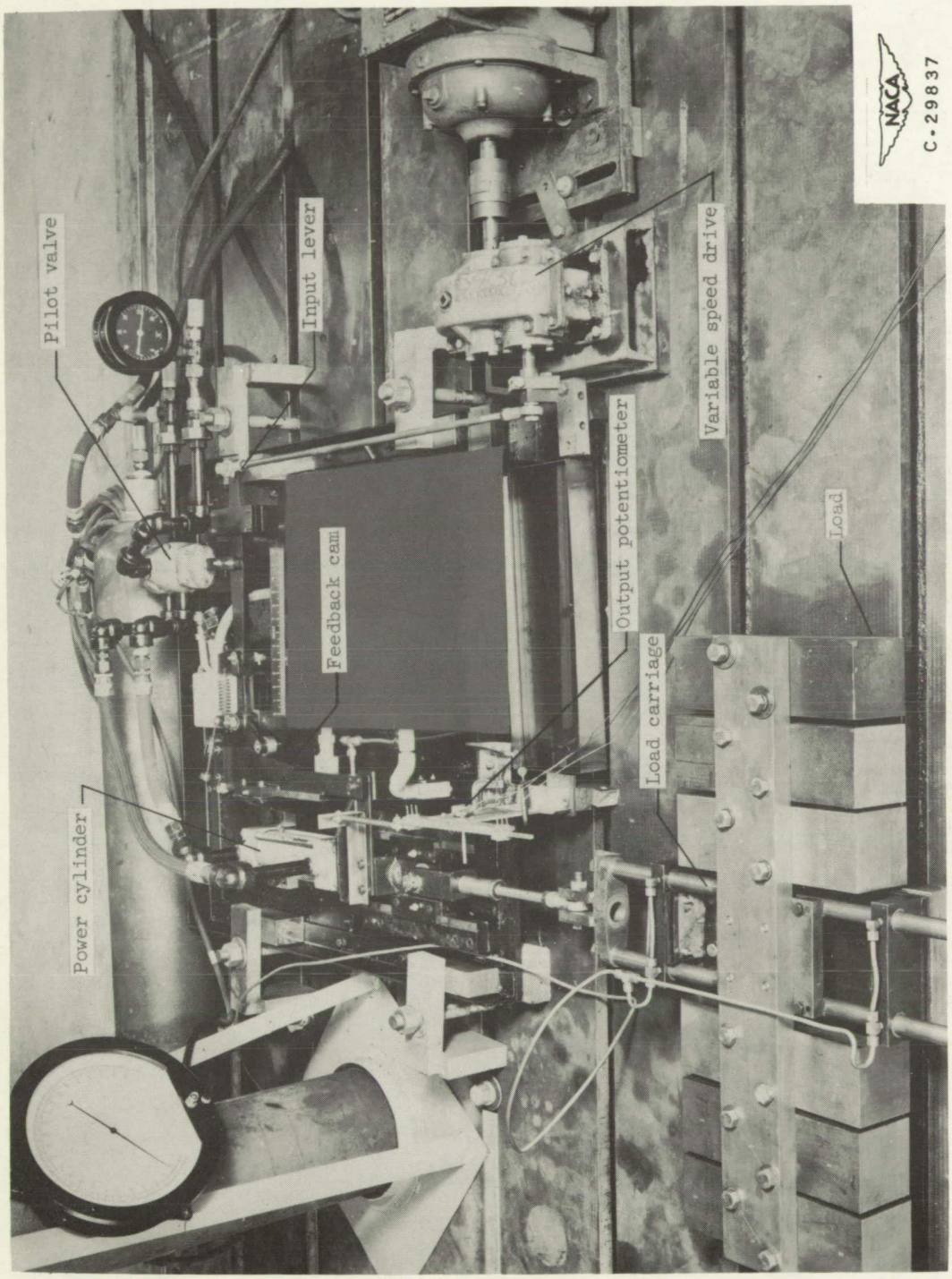


Figure 16. - Straight-line hydraulic servomotor instrumented for recording response to a sinusoidally varying input.

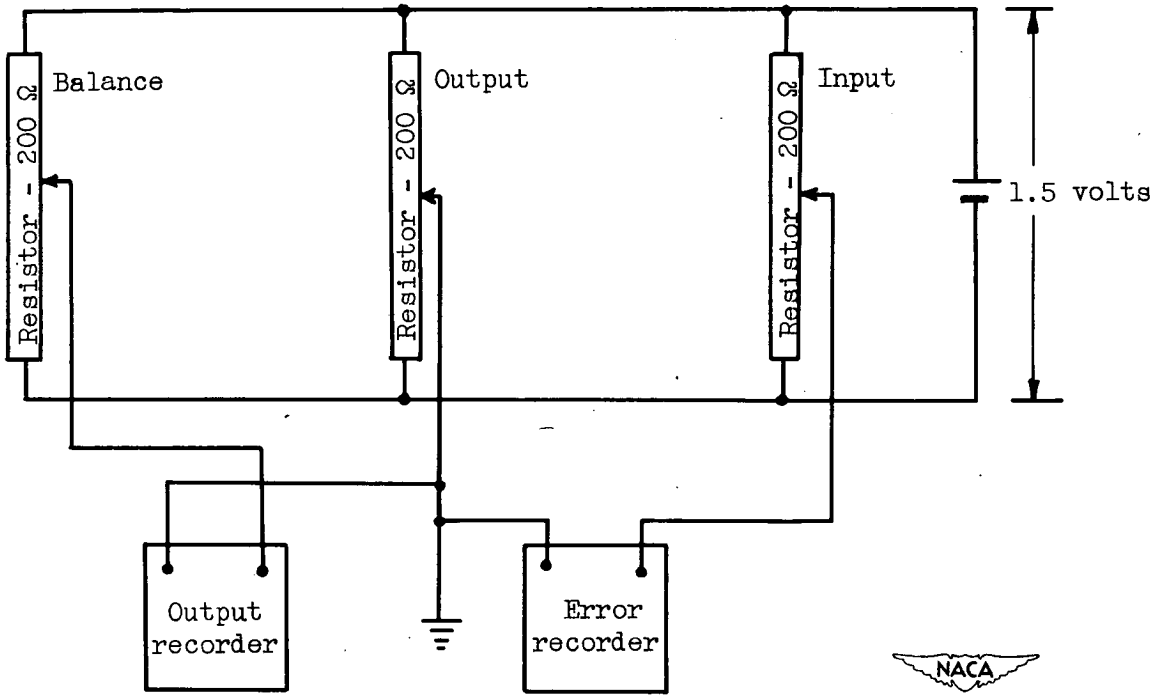


Figure 17. - Instrumentation for determining frequency-response characteristics of hydraulic servomotor.

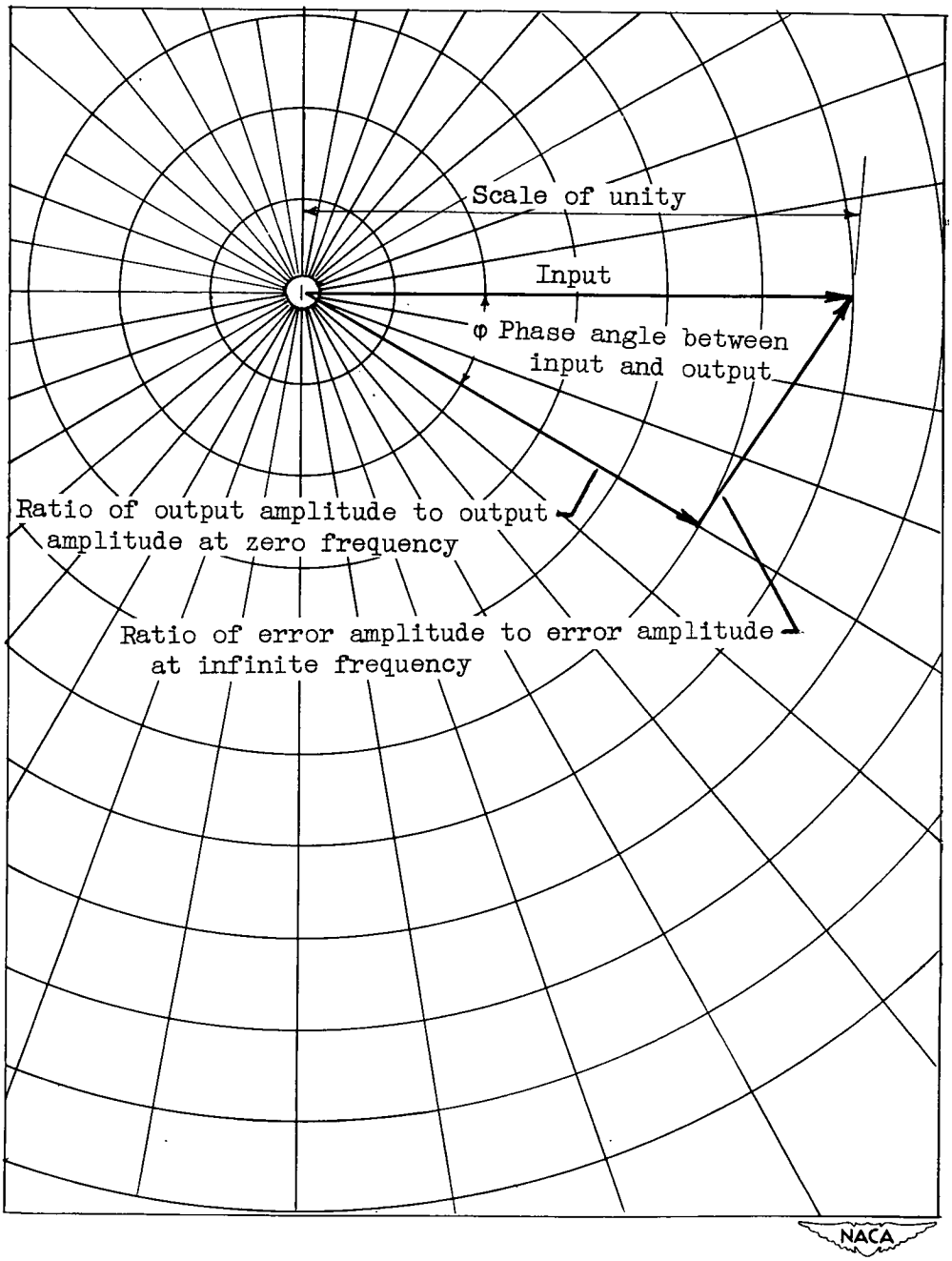


Figure 18. - Diagram for determination of phase angle from frequency-response data.